catalysts

MDPI

Electronic Supplementary Information

Ring Opening Polymerization of Lactides and Lactones by Multimetallic Titanium Complexes Derived from the Acids $Ph_2C(X)CO_2H$ (X = OH, NH_2)

Xin Zhang [1], Timothy J. Prior [1], Kai Chen [2], Orlando Santoro [1,3] and Carl Redshaw [1,*]

[1] Plastics Collaboratory, Department of Chemistry, University of Hull, Cottingham Road, Hull HU6 7RX, UK
[2] Collaborative Innovation Center of Atmospheric Environment and Equipment Technology, Jiangsu Key Laboratory of Atmospheric Environment Monitoring and Pollution Control, School of Environmental Science and Engineering, Nanjing University of Information Science & Technology, Nanjing 210044, China
[3] Dipartimento di Biotecnologie e Scienze della Vita, Università degli Studi dell'Insubria, 21100 Varese, Italy
* Correspondence: c.redshaw@hull.ac.uk

Contents

Figure S1. Harris notation and its application in describing these ligands.
Figure S2. Alternative view of **1**.
Figure S3. Coordination about the two independent Ti ions in **2**.
Figure S4. Alternate view (ORTEP) of **3** with atoms drawn as 25 % probability ellipsoids. Minor disorder and hydrogen atoms are omitted for clarity.
Figure S5. Asymmetric unit of **4** with atoms drawn as spheres of arbitrary radius. Each disorder component is illustrated; hydrogen atoms are not shown for clarity.
Figure S6. Alternative view of **5** with atoms drawn as 50% probability ellipsoids. For clarity hydrogen atoms have been omitted.
Figure S7. View of the crystal structure of **6** down *a*. Dashed lines show hydrogen bonds.
Figure S8. The two unique complexes in **7** composed of Ti1 and Ti2. Symmetry-equivalent atoms are generated by the following symmetry operations: $1 = 1–x, 2–y, 2–z; $2 = –x, 1–y, 1–z.
Figure S9. Two Ti cluster present in **8**. Symmetry operation used to generate equivalent atoms: i = 1–*x*, 1–*y*, 1–*z*.
Figure S10. Asymmetric unit of **9**. A portion of the infinite hydrogen bonded chain running parallel to the crystallographic *a* direction (left-right on the image) is shown as dashed lines.
Figure S11. Hydrogen-bonded chain within **10**. Dashed lines show hydrogen bonds.
Figure S12. ^{1}H NMR (400 MHz, $CDCl_3$) spectrum of PCL using **1** (Table 1, entry 1).
Figure S13. MALDI-TOF spectrum of PCL using **1** (Table 1, entry 1).
Figure S14. ^{1}H NMR (400 MHz, $CDCl_3$) spectrum of PCL using **2** (Table 1, entry 2).
Figure S15. MALDI-TOF spectrum of PCL using **2** (Table 1, entry 2).
Figure S16. ^{1}H NMR (400 MHz, $CDCl_3$) spectrum of PCL using **3** (Table 1, entry 3).
Figure S17. MALDI-TOF spectrum of PCL using **3** (Table 1, entry 3).
Figure S18. ^{1}H NMR (400 MHz, $CDCl_3$) spectrum of PCL using **4** (Table 1, entry 4).
Figure S19. MALDI-TOF spectrum of PCL using **4** (Table 1, entry 4).

Figure S20. ^{1}H NMR (400 MHz, $CDCl_3$) spectrum of PCL using **5** (Table 1, entry 5).

Figure S21. MALDI-TOF spectrum of PCL using **5** (Table 1, entry 5).

Figure S22. ^{1}H NMR (400 MHz, $CDCl_3$) spectrum of PCL using **6** (Table 1, entry 6).

Figure S23. MALDI-TOF spectrum of PCL using **6** (Table 1, entry 6).

Figure S24. ^{1}H NMR (400 MHz, $CDCl_3$) spectrum of PCL using **7** (Table 1, entry 7).

Figure S25. MALDI-TOF of PCL using **7** (Table 1, entry 7).

Figure S26. ^{1}H NMR (400 MHz, $CDCl_3$) spectrum of PCL using **9** (Table 1, entry 9).

Figure S27. MALDI-TOF of PCL using **9** (Table 1, entry 9).

Figure S28. ^{1}H NMR (400 MHz, $CDCl_3$) spectrum of PCL using **10** (Table 1, entry 10).

Figure S29. MALDI-TOF spectrum of PCL using **10** (Table 1, entry 10).

Figure S30. 3D time-resolved ^{1}H NMR (400 MHz, toluene-d_8) of kinetics of *r*-LA using complex **7** (Table 3, entry 7).

Figure S31. ^{1}H NMR (400 MHz, $CDCl_3$) spectrum of PLA using **1** (Table 3, entry 1).

Figure S32. MALDI-TOF spectrum of PLA using **1** (Table 3, entry 1).

Figure S33. ^{1}H NMR (400 MHz, $CDCl_3$) spectrum of PLA using **2** (Table 3, entry 2).

Figure S34. MALDI-TOF spectrum of PLA using **2** (Table 3, entry 2).

Figure S35. MALDI-TOF spectrum of PLA using **3** (Table 3, entry 3).

Figure S36. ^{1}H NMR (400 MHz, $CDCl_3$) spectrum of PLA using **4** (Table 3, entry 4).

Figure S37. MALDI-TOF spectrum of PLA using **4** (Table 3, entry 4).

Figure S38. MALDI-TOF spectrum of PLA using **5** (Table 3, entry 5).

Figure S39. ^{1}H NMR (400 MHz, $CDCl_3$) spectrum of PLA using **7** (Table 3, entry 7).

Figure S40. MALDI-TOF spectrum of PLA using **7** (Table 3, entry 7).

Figure S41. ^{1}H NMR (400 MHz, $CDCl_3$) spectrum of PLA using **8** (Table 3, entry 8).

Figure S42. MALDI-TOF spectrum of PLA using **8** (Table 3, entry 8).

Figure S43. ^{1}H NMR (400 MHz, $CDCl_3$) spectrum of PLA using **9** (Table 3, entry 9).

Figure S44. MALDI-TOF spectrum of PLA using **9** (Table 3, entry 9).

Figure S45. ^{13}C NMR spectrum of methine carbon in PLA using **1** (left) and **2** (right) (Table 3, entries 1 and 2).

Figure S46. ^{13}C NMR spectrum of methine carbon in PLA using **3** (left) and **4** (right) (Table 3, entries 3 and 4).

Figure S47. ^{13}C NMR spectrum of methine carbon in PLA using **5** (left) and **6** (right) (Table 3, entries 5 and 6).

Figure S48. ^{13}C NMR spectrum of methine carbon in PLA using **7** (left) and **8** (right) (Table 3, entries 7 and 8).

Figure S49. ^{13}C NMR spectrum of methine carbon in PLA using **9** (left) and **10** (right) (Table 3, entries 9 and 10).

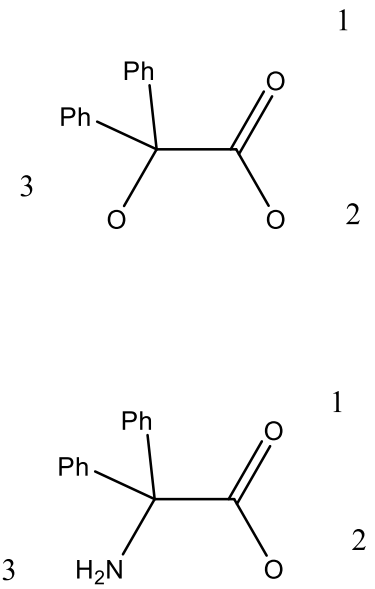

Figure S1. Harris notation and its application in describing these ligands.

In line with the method of Harris, [S1] we have described the coordination of the benzilic acid in a systematic way. We have numbered each of the oxygen atoms in a consistent manner as shown above. The order in the Harris symbol reflects the binding of each atom in order. For example, [2.021] signifies the ligand binds to two metals, oxygen #1 does not bind, oxygen #2 binds to both metal ions, and oxygen #3 binds to one metal. It is notable that the same binding occurs for diphenyl glycine in each case, namely [1.011]. That is to say the dpg is chelating through O#2 and N#3.
In some cases it is necessary to remove ambiguity about which metal ions are bound and this is done through the use of subscripts to identify the metal ions. For example, [$3.1_1 1_2 2_{13}$] would signify three unique bound metal ions; atom 1 binds M#1, atom 2 binds M#2, and atom 3 binds both M#1 and M#3.

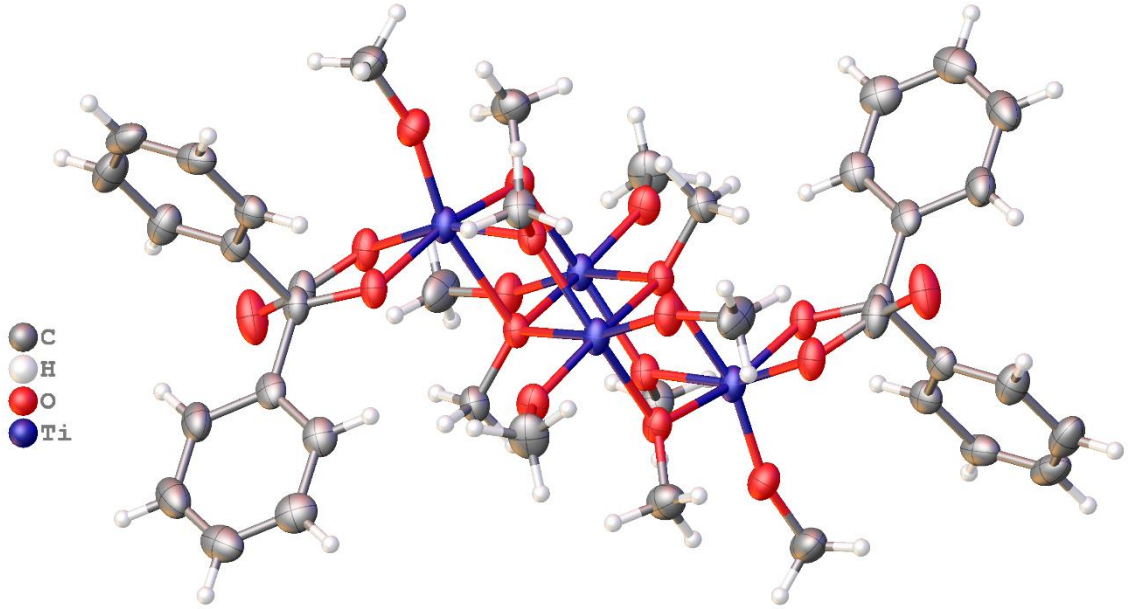

Figure S2. Alternative view of **1**.

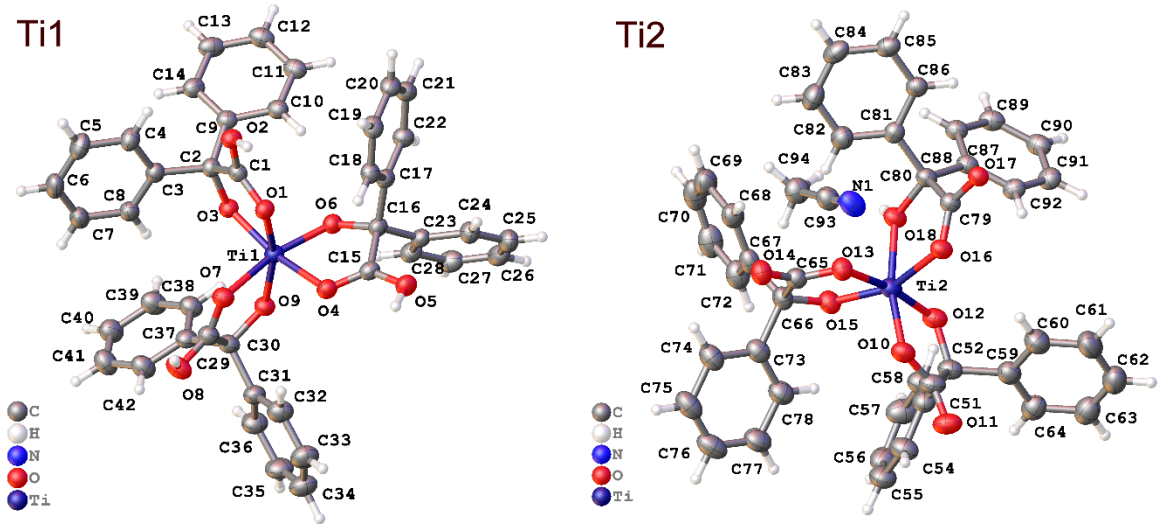

Figure S3. Coordination about the two independent Ti ions in **2**.

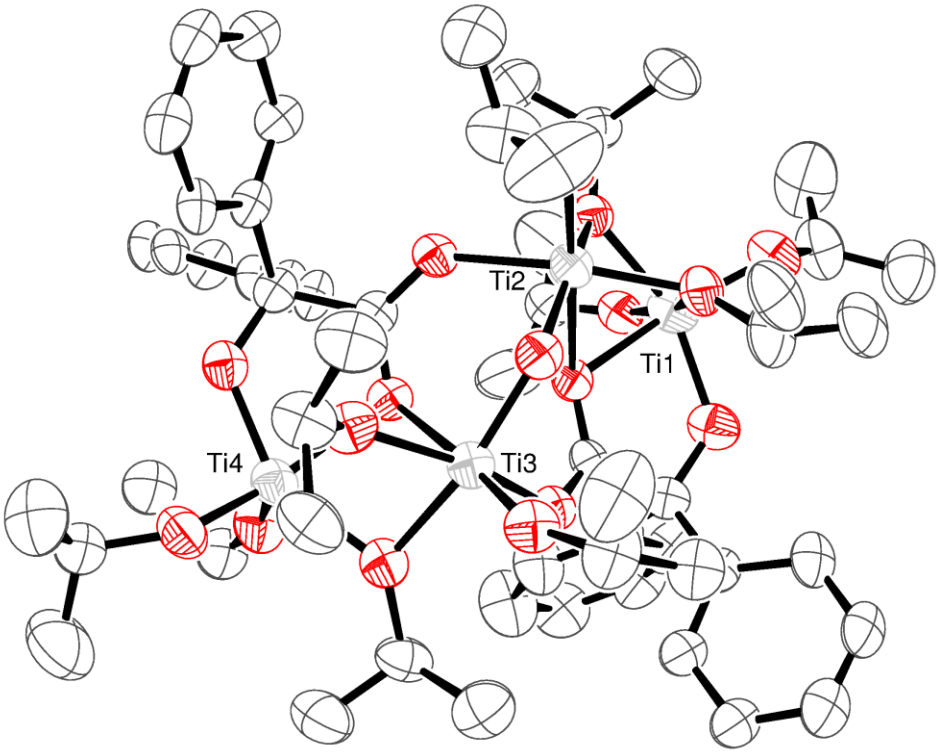

Figure S4. Alternate view (ORTEP) of **3** with atoms drawn as 25 % probability ellipsoids. Minor disorder and hydrogen atoms are omitted for clarity.

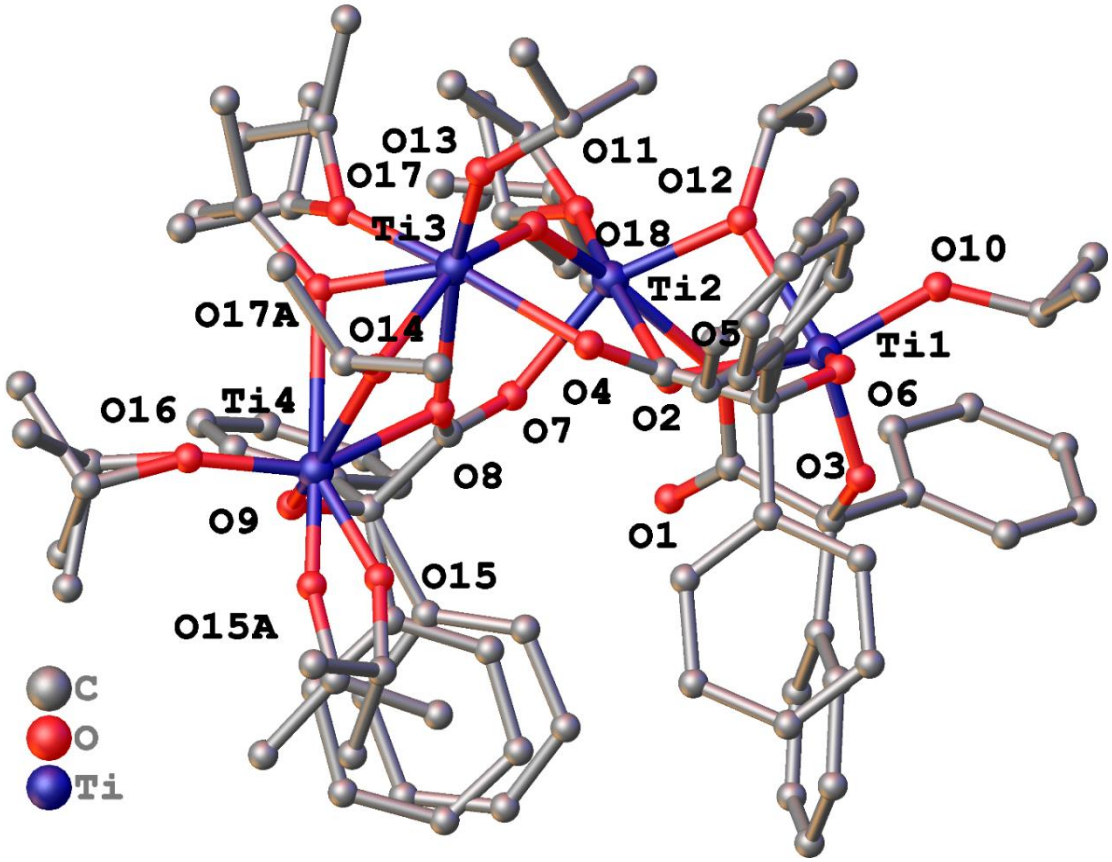

Figure S5. Asymmetric unit of **4** with atoms drawn as spheres of arbitrary radius. Each disorder component is illustrated; hydrogen atoms are not shown for clarity.

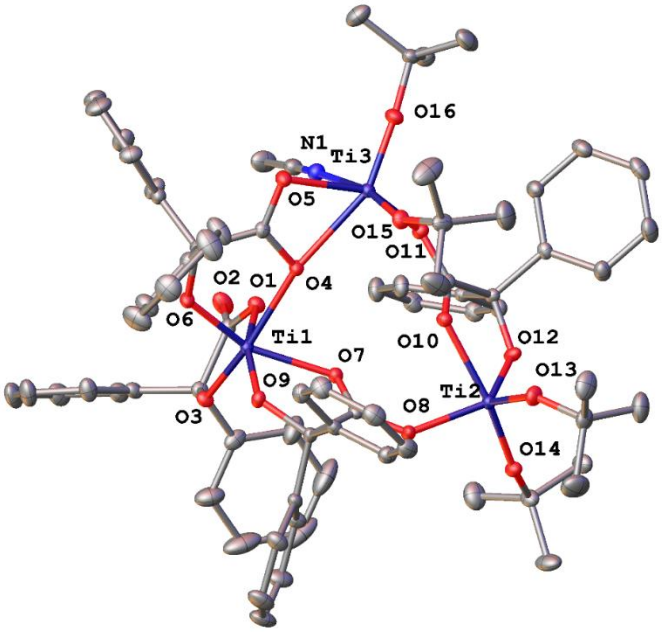

Figure S6. Alternative view of **5** with atoms drawn as 50% probability ellipsoids. For clarity hydrogen atoms have been omitted.

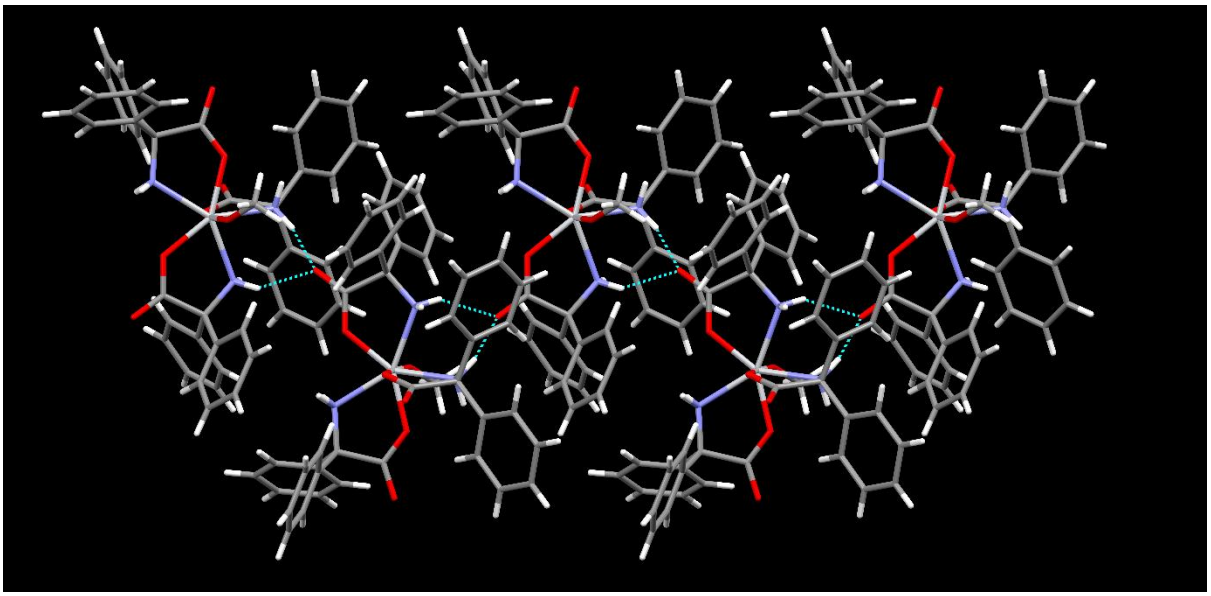

Figure S7. View of the crystal structure of **6** down *a*. Dashed lines show hydrogen bonds.

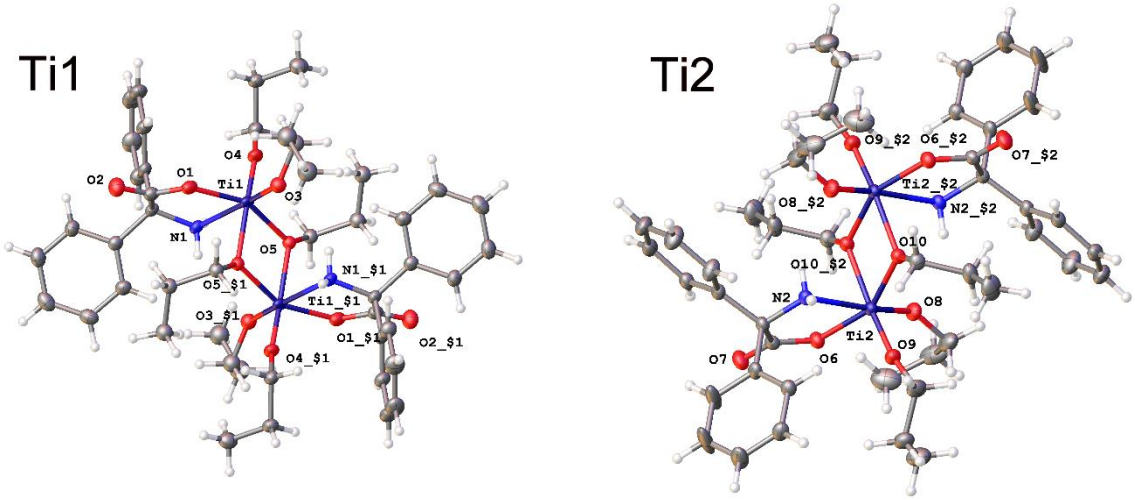

Figure S8. The two unique complexes in **7** composed of Ti1 and Ti2. Symmetry-equivalent atoms are generated by the following symmetry operations: $1 = 1–x, 2–y, 2–z; $2 = –x, 1–y, 1–z.

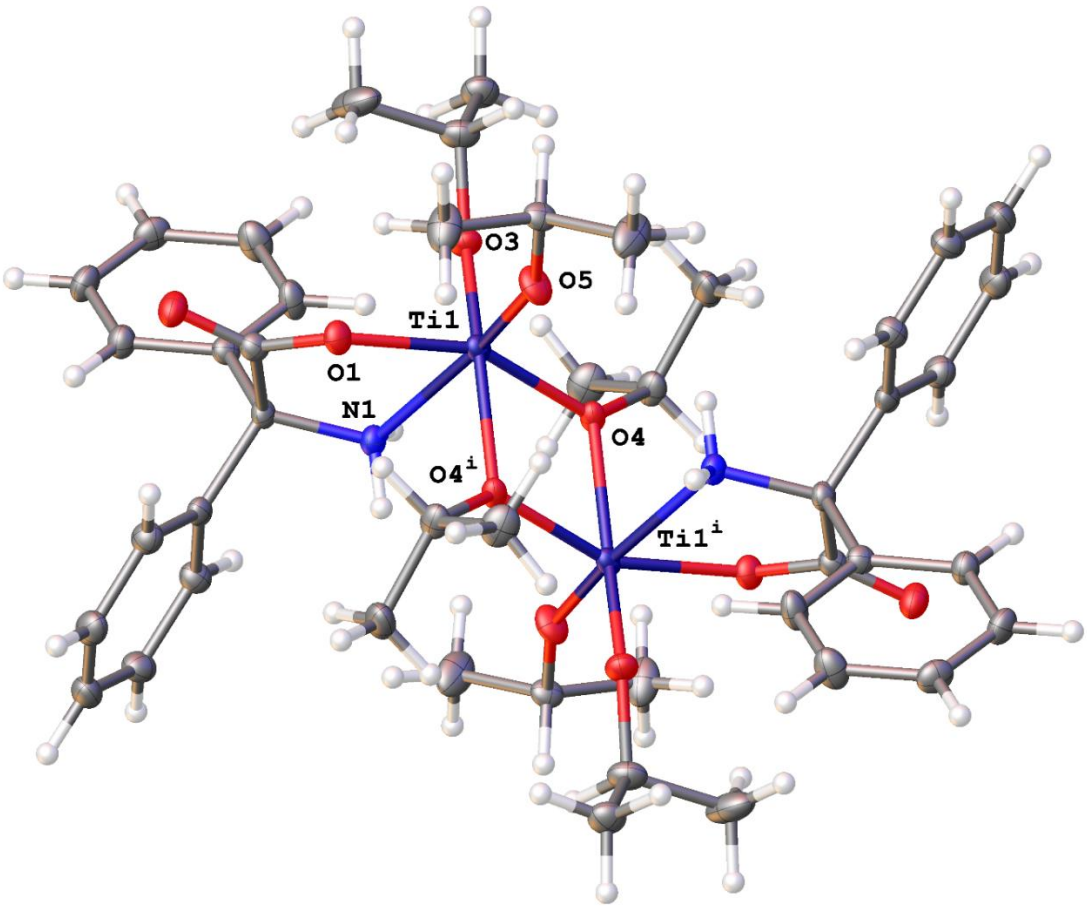

Figure S9. Two Ti cluster present in **8**. Symmetry operation used to generate equivalent atoms: i = 1–*x*, 1–*y*, 1–*z*.

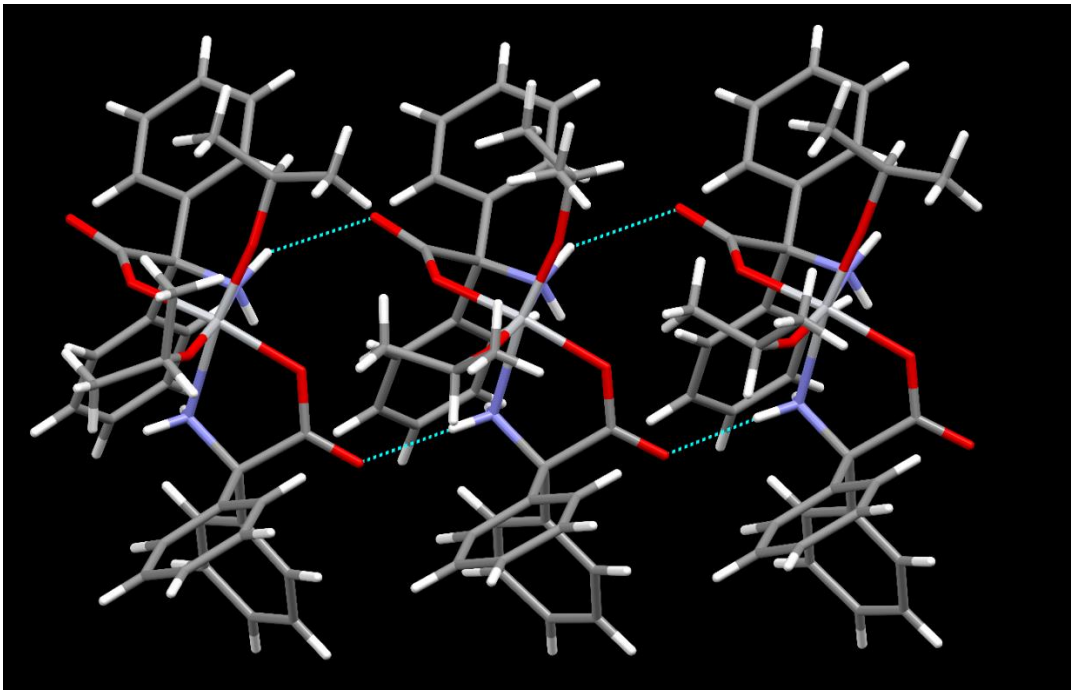

Figure S10. Asymmetric unit of **9**. A portion of the infinite hydrogen bonded chain running parallel to the crystallographic *a* direction (left-right on the image) is shown as dashed lines.

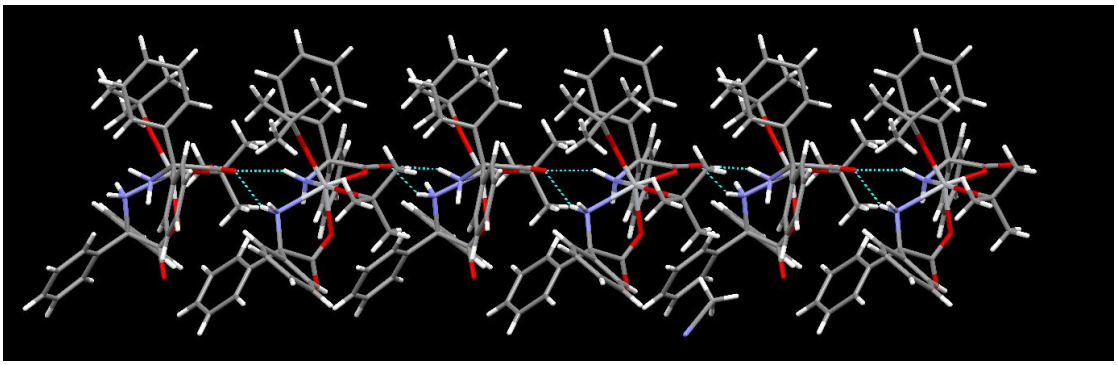

Figure S11. Hydrogen-bonded chain within **10**. Dashed lines show hydrogen bonds.

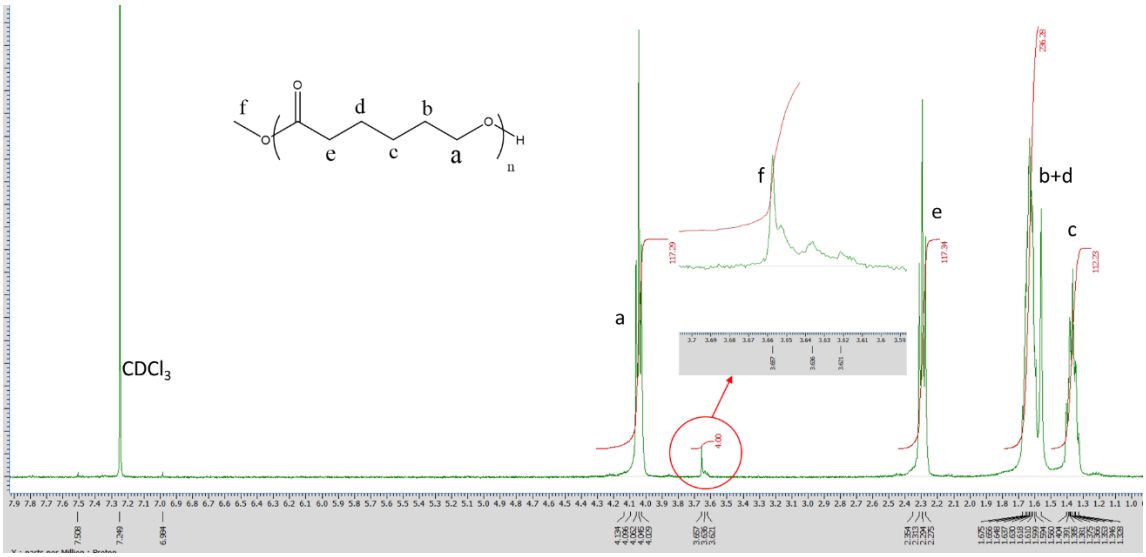

Figure S12. ^{1}H NMR (400 MHz, $CDCl_3$) spectrum of PCL using **1** (Table 1, entry 1).

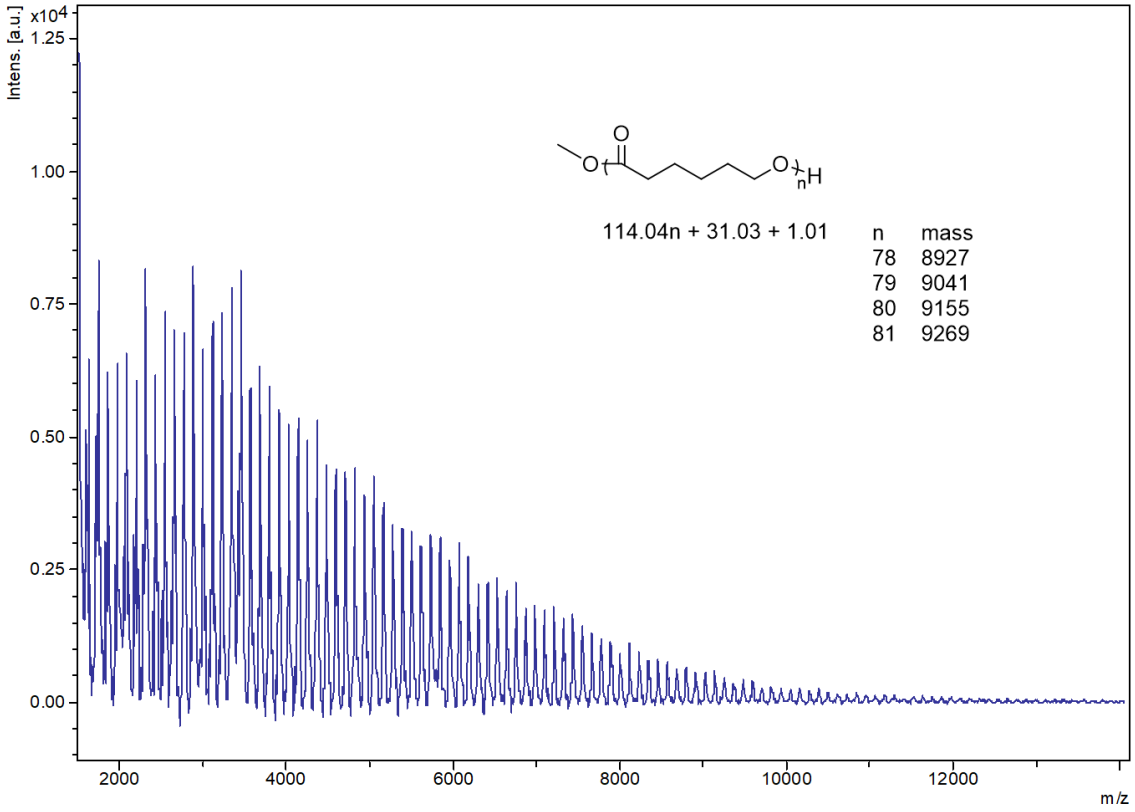

Figure S13. MALDI-TOF spectrum of PCL using **1** (Table 1, entry 1).

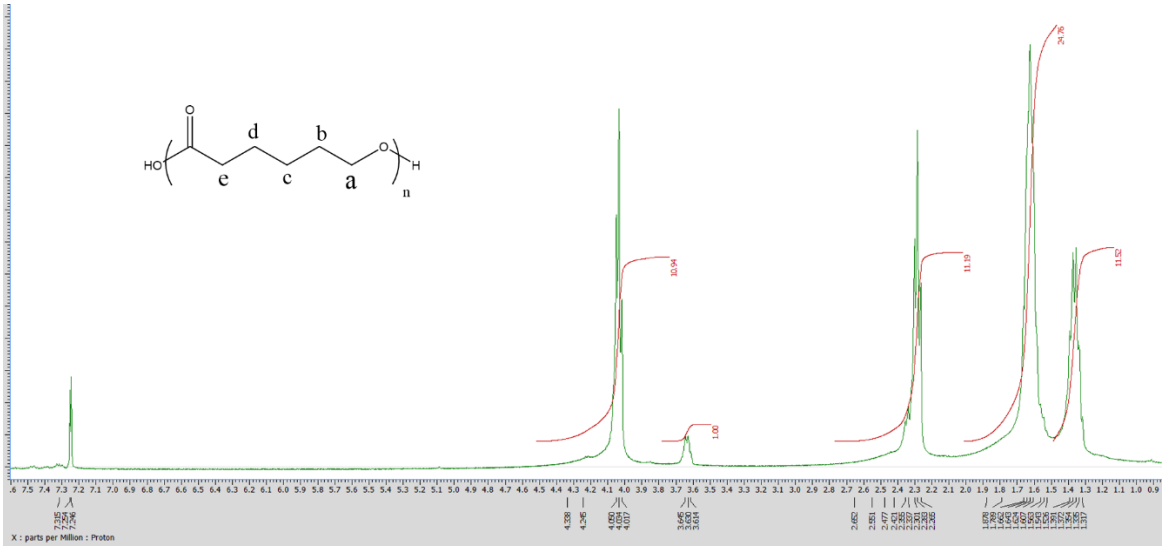

Figure S14. ^{1}H NMR (400 MHz, $CDCl_3$) spectrum of PCL using **2** (Table 1, entry 2).

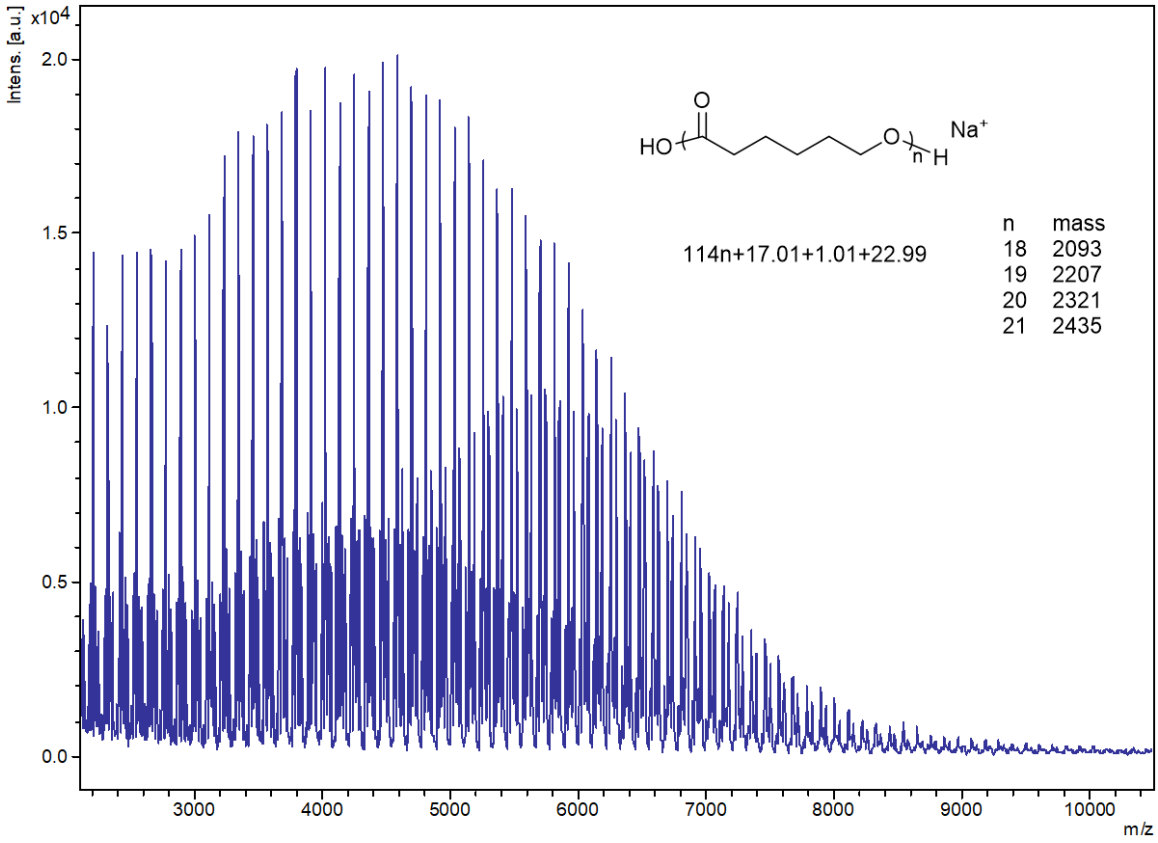

Figure S15. MALDI-TOF spectrum of PCL using **2** (Table 1, entry 2).

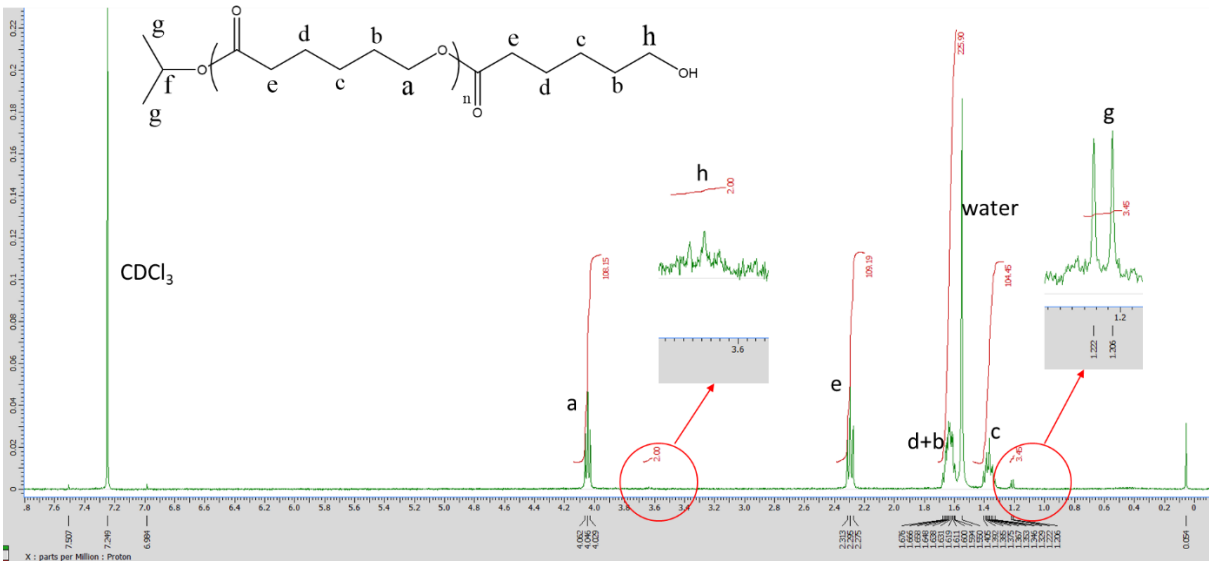

Figure S16. ^{1}H NMR (400 MHz, $CDCl_3$) spectrum of PCL using **3** (Table 1, entry 3).

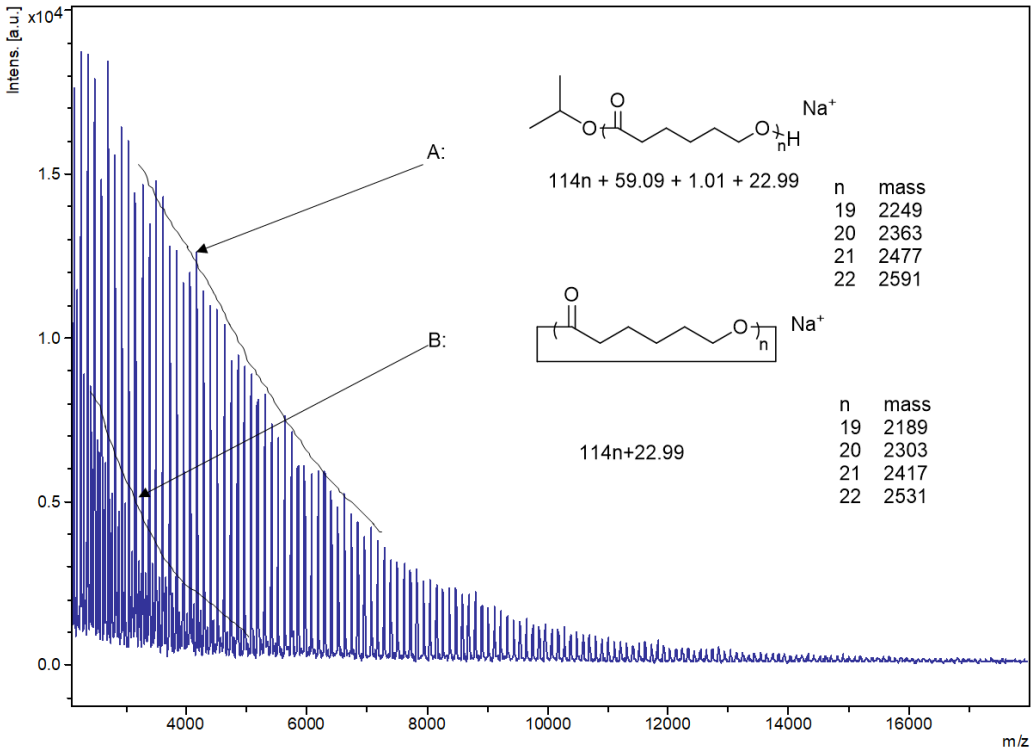

Figure S17. MALDI-TOF spectrum of PCL using **3** (Table 1, entry 3).

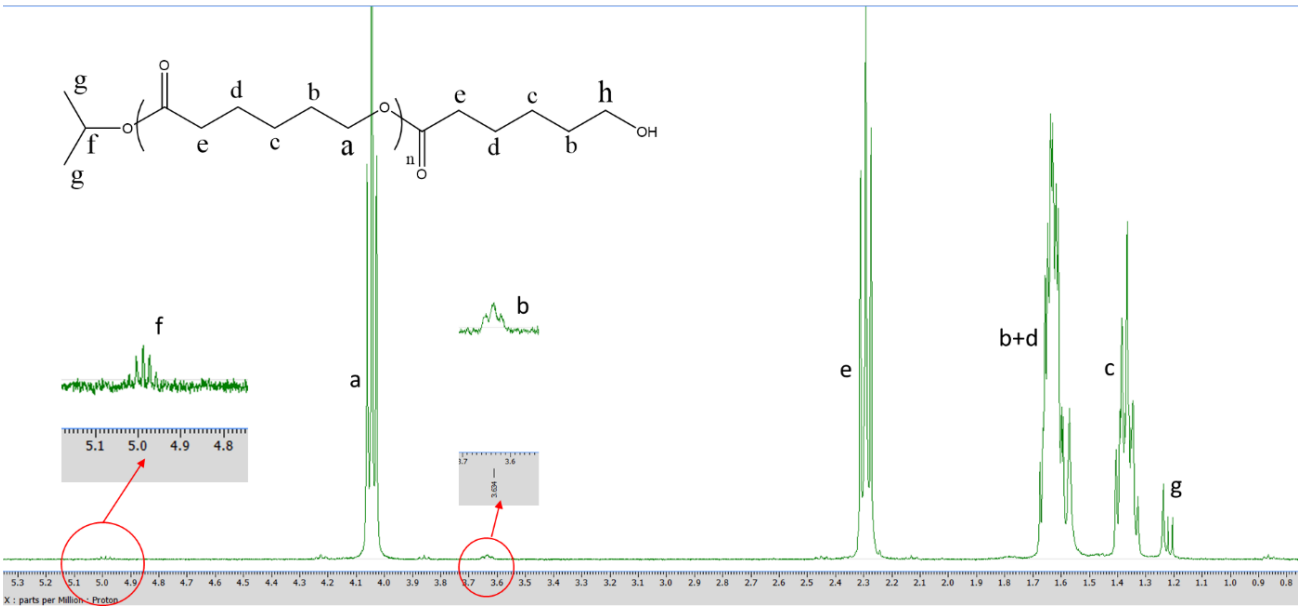

Figure S18. ^{1}H NMR (400 MHz, $CDCl_3$) spectrum of PCL using **4** (Table 1, entry 4).

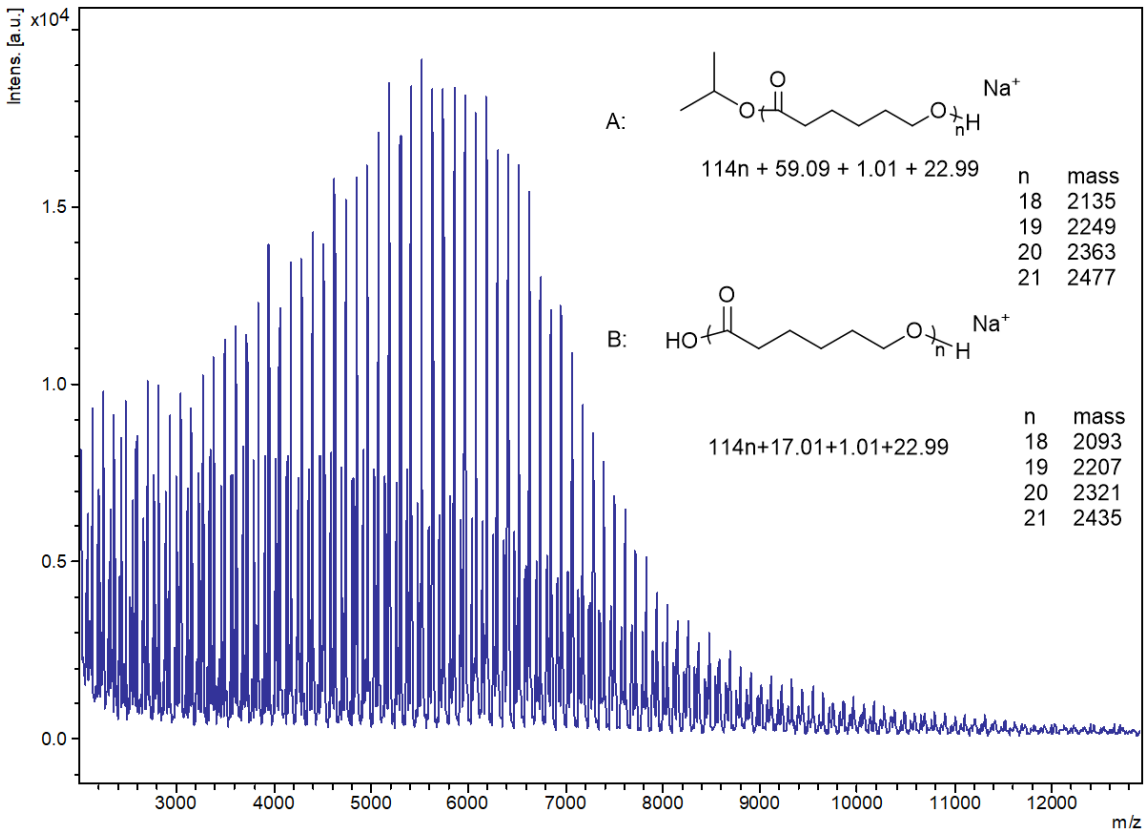

Figure S19. MALDI-TOF spectrum of PCL using **4** (Table 1, entry 4).

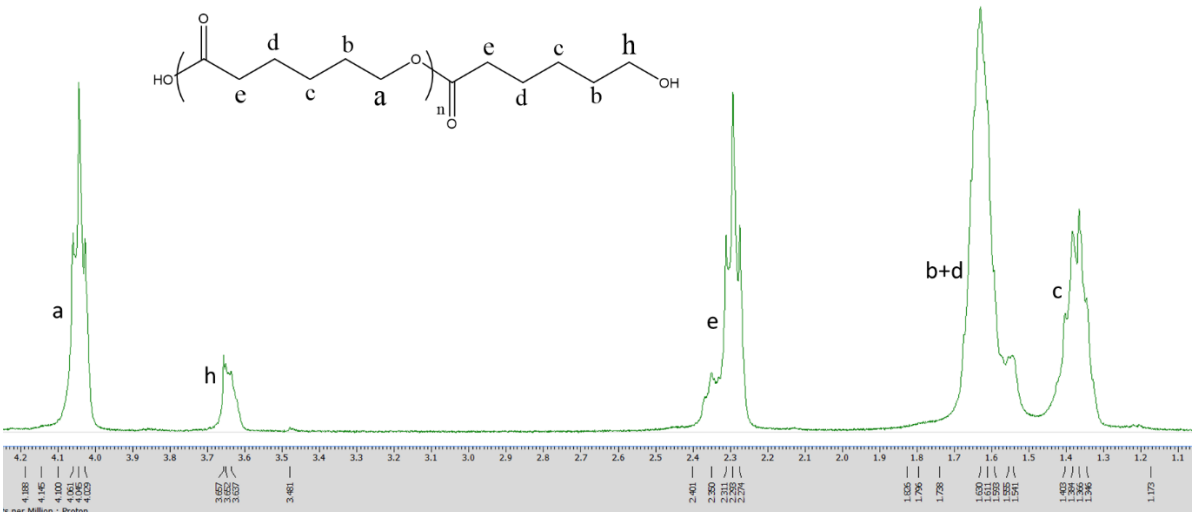

Figure S20. ^{1}H NMR (400 MHz, $CDCl_3$) spectrum of PCL using **5** (Table 1, entry 5).

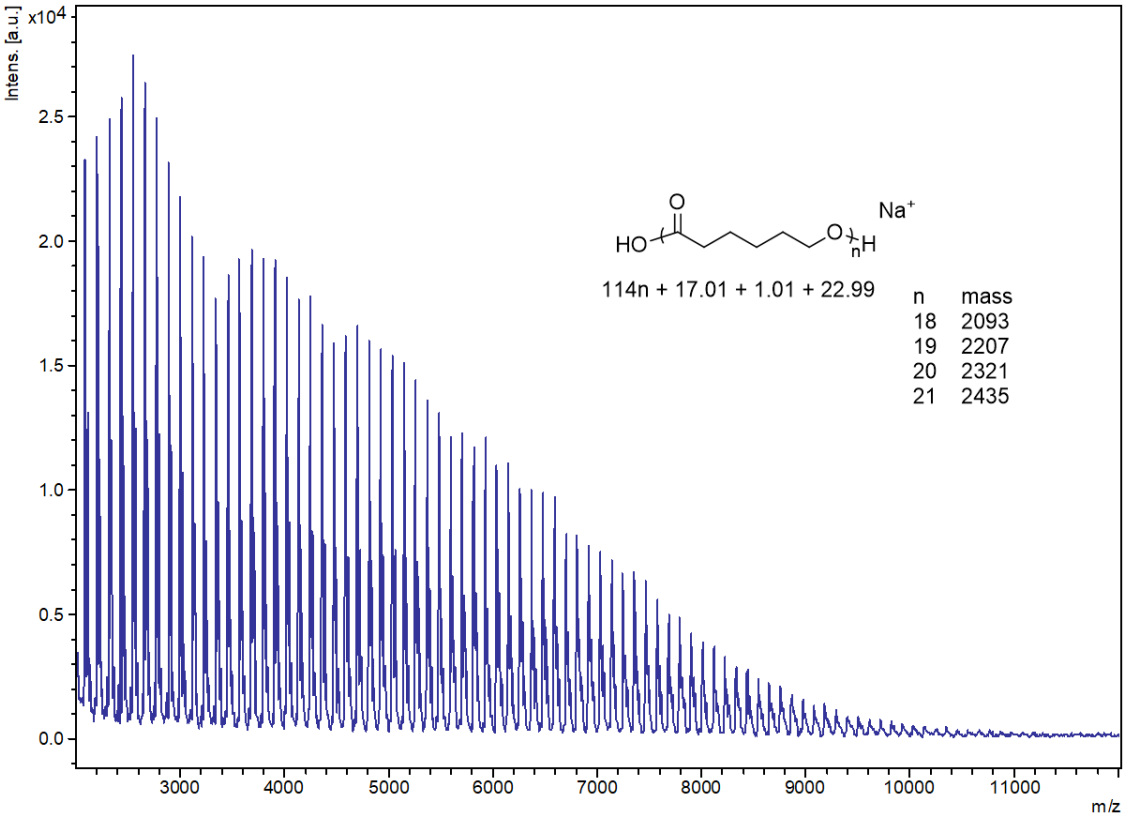

Figure S21. MALDI-TOF spectrum of PCL using **5** (Table 1, entry 5).

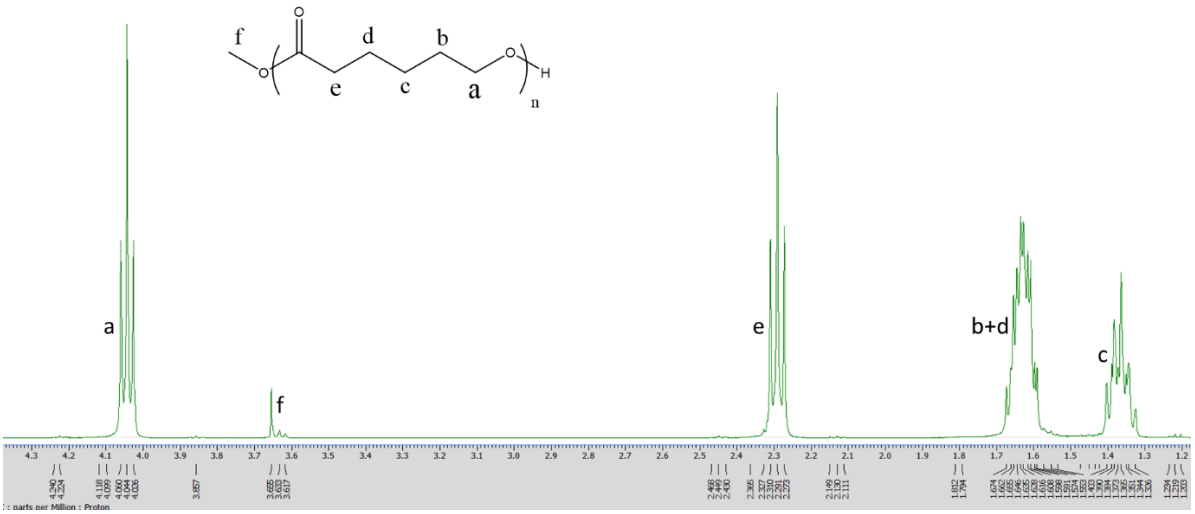

Figure S22. ^{1}H NMR (400 MHz, $CDCl_3$) spectrum of PCL using **6** (Table 1, entry 6).

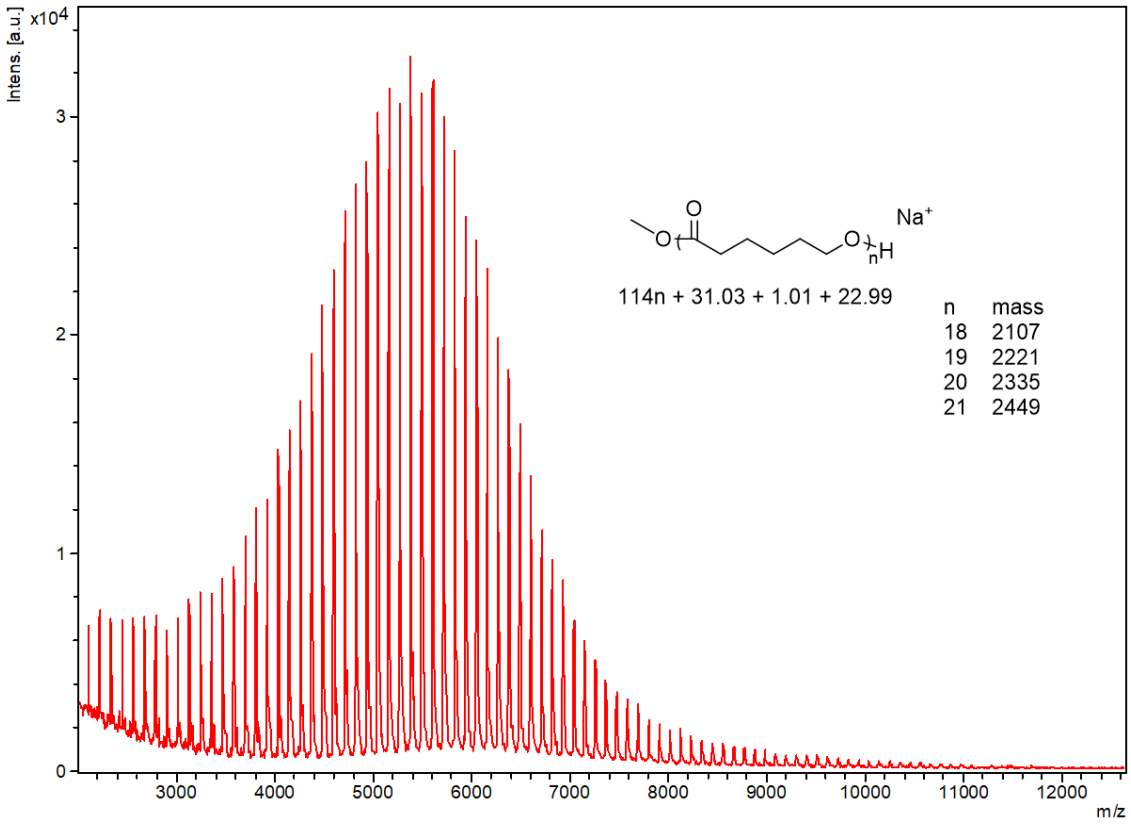

Figure S23. MALDI-TOF spectrum of PCL using **6** (Table 1, entry 6).

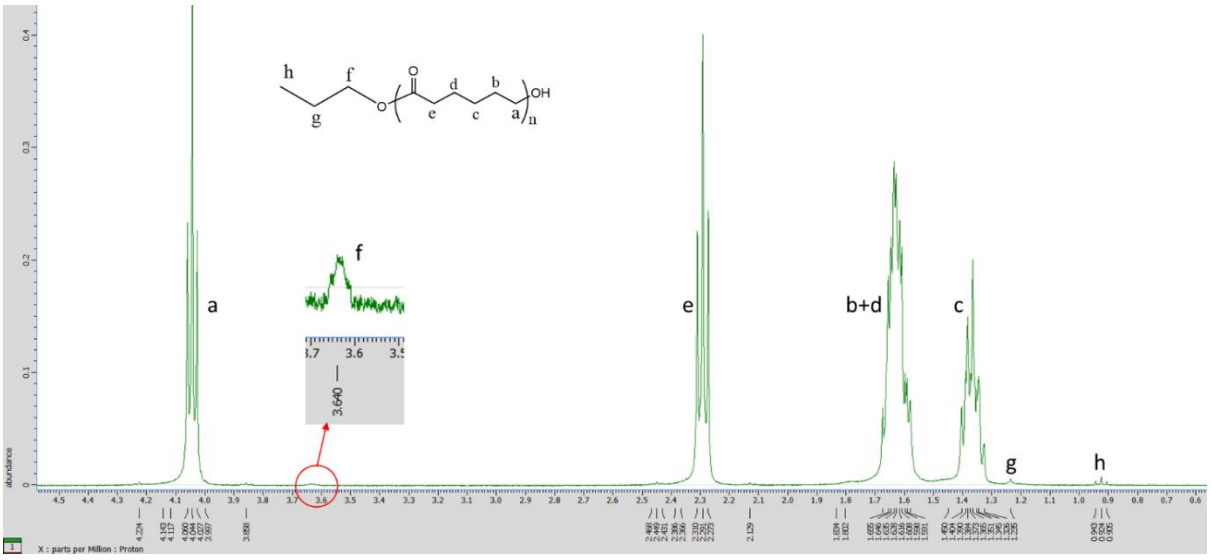

Figure S24. ^{1}H NMR (400 MHz, $CDCl_3$) spectrum of PCL using **7** (Table 1, entry 7).

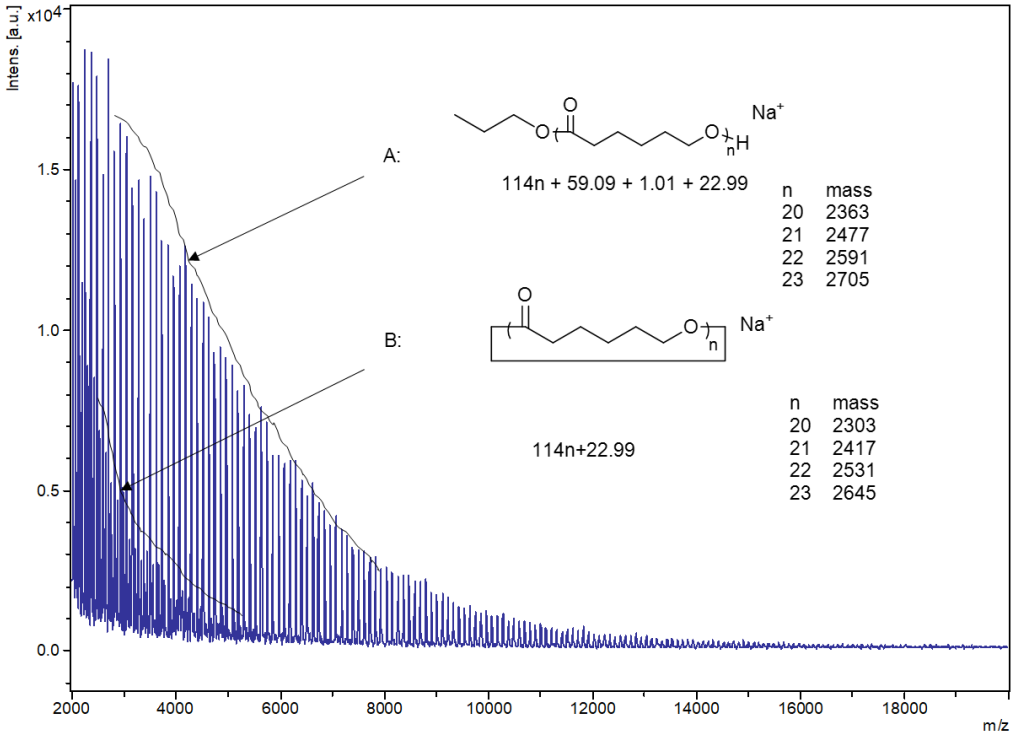

Figure S25. MALDI-TOF of PCL using **7** (Table 1, entry 7).

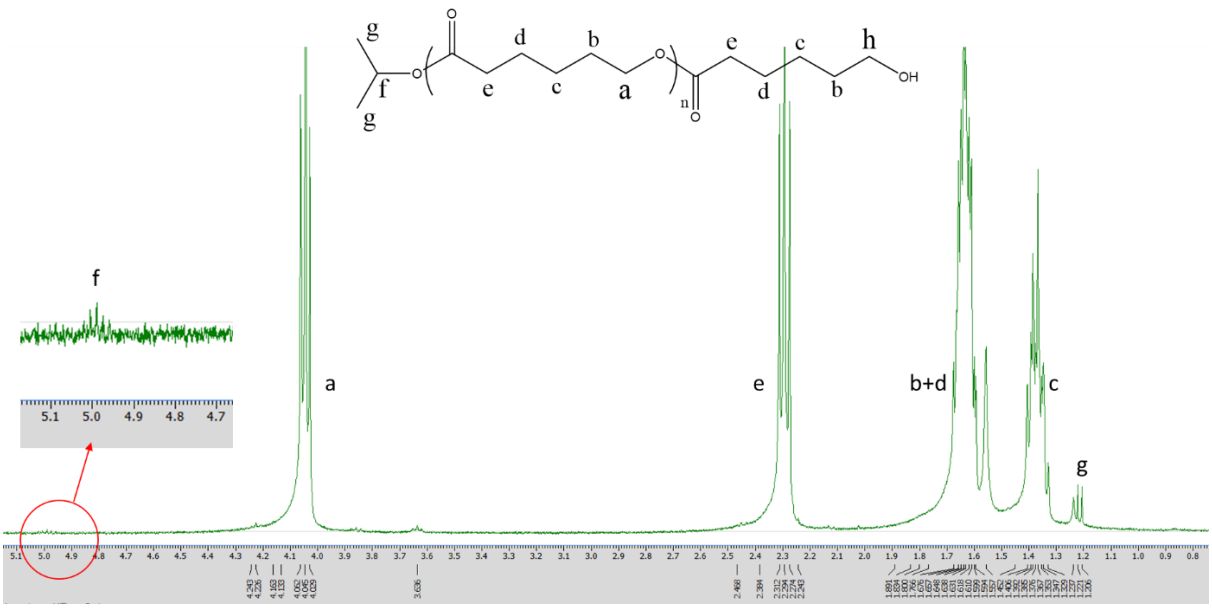

Figure S26. ^{1}H NMR (400 MHz, $CDCl_3$) spectrum of PCL using **9** (Table 1, entry 9).

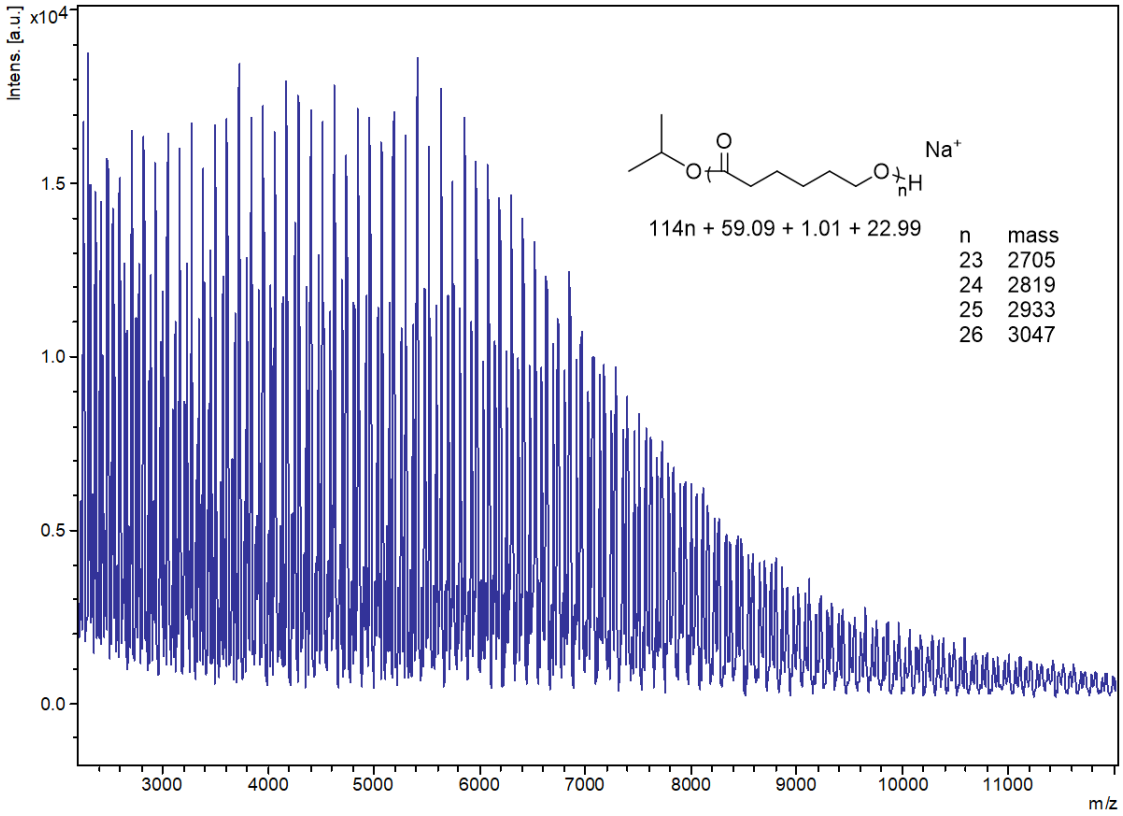

Figure S27. MALDI-TOF of PCL using **9** (Table 1, entry 9).

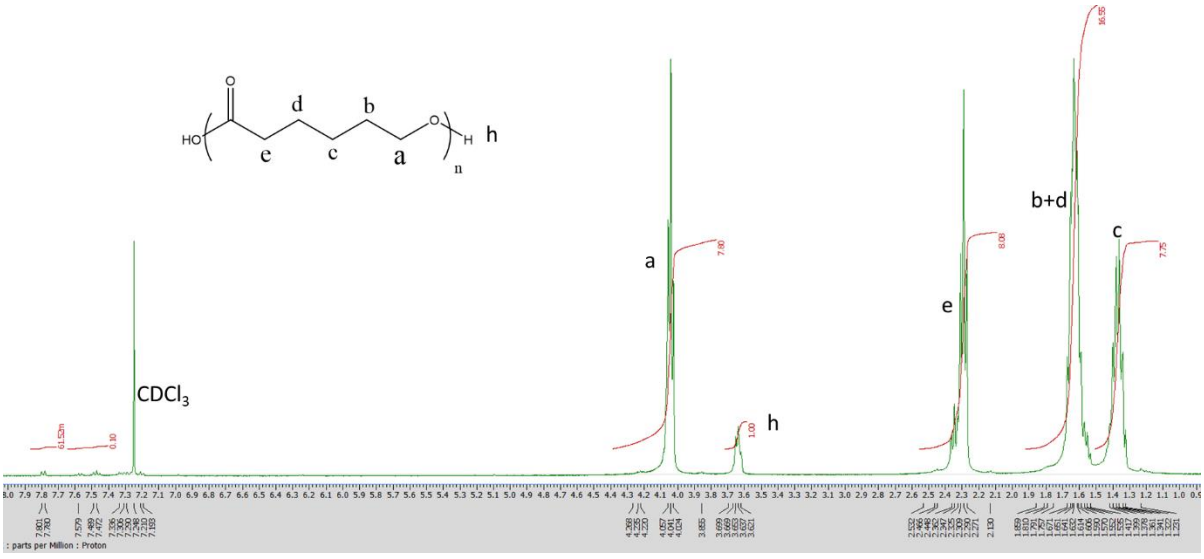

Figure S28. ^{1}H NMR (400 MHz, $CDCl_3$) spectrum of PCL using **10** (Table 1, entry 10).

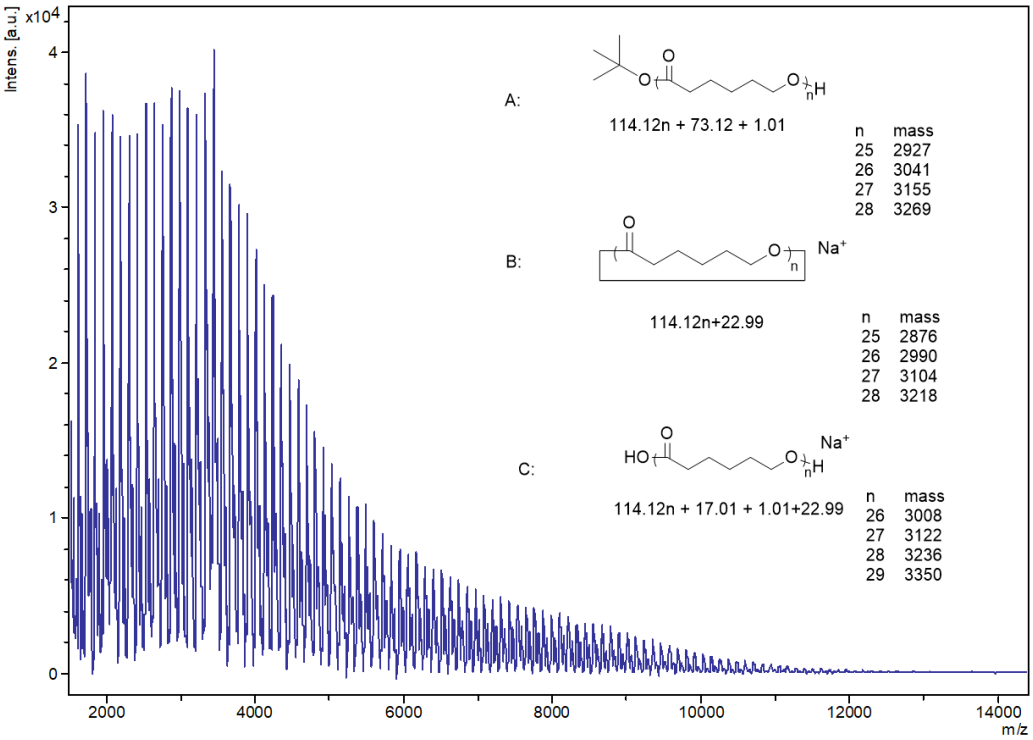

Figure S29. MALDI-TOF spectrum of PCL using **10** (Table 1, entry 10).

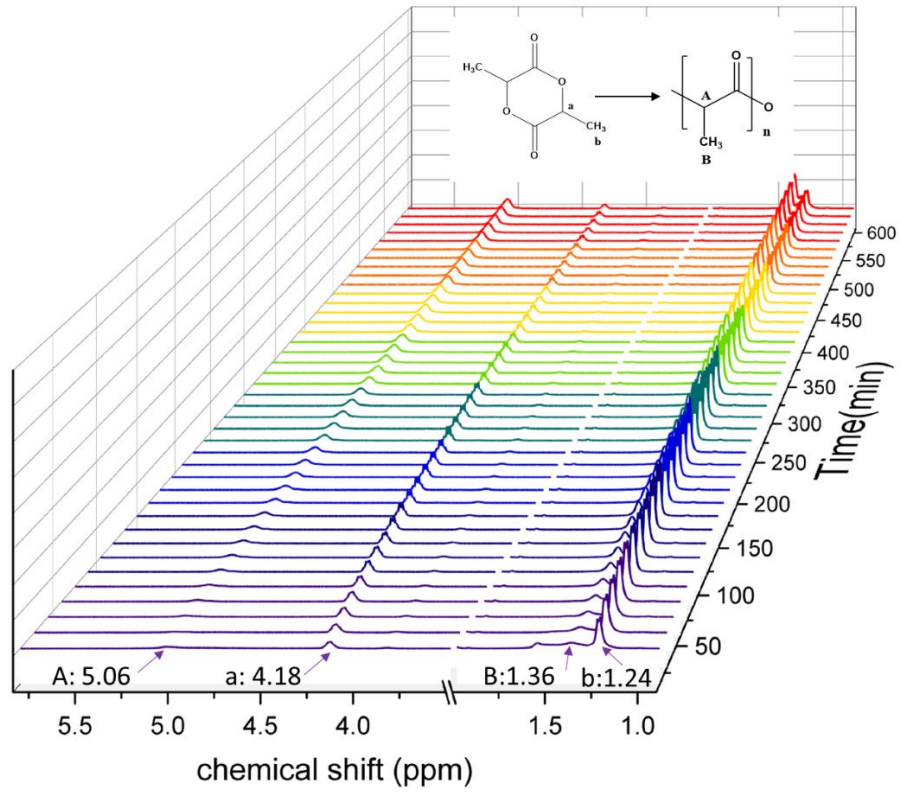

Figure S30. 3D time-resolved ^{1}H NMR (400 MHz, toluene-d$_8$) of kinetics of *r*-LA using complex **7** (Table 3, entry 7).

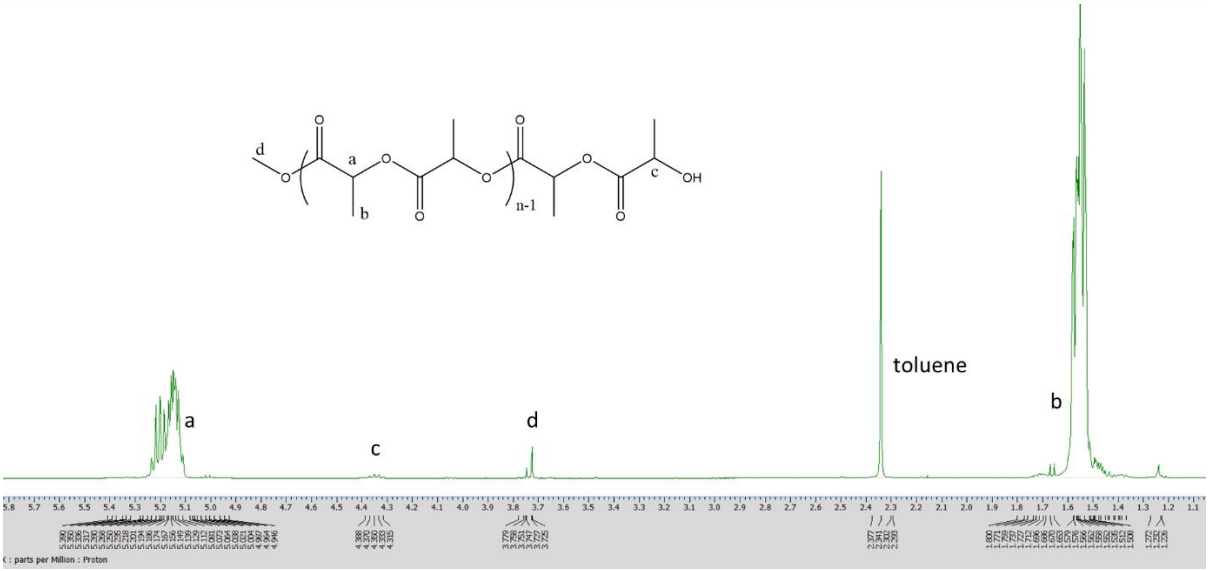

Figure S31. ^{1}H NMR (400 MHz, $CDCl_3$) spectrum of PLA using **1** (Table 3, entry 1).

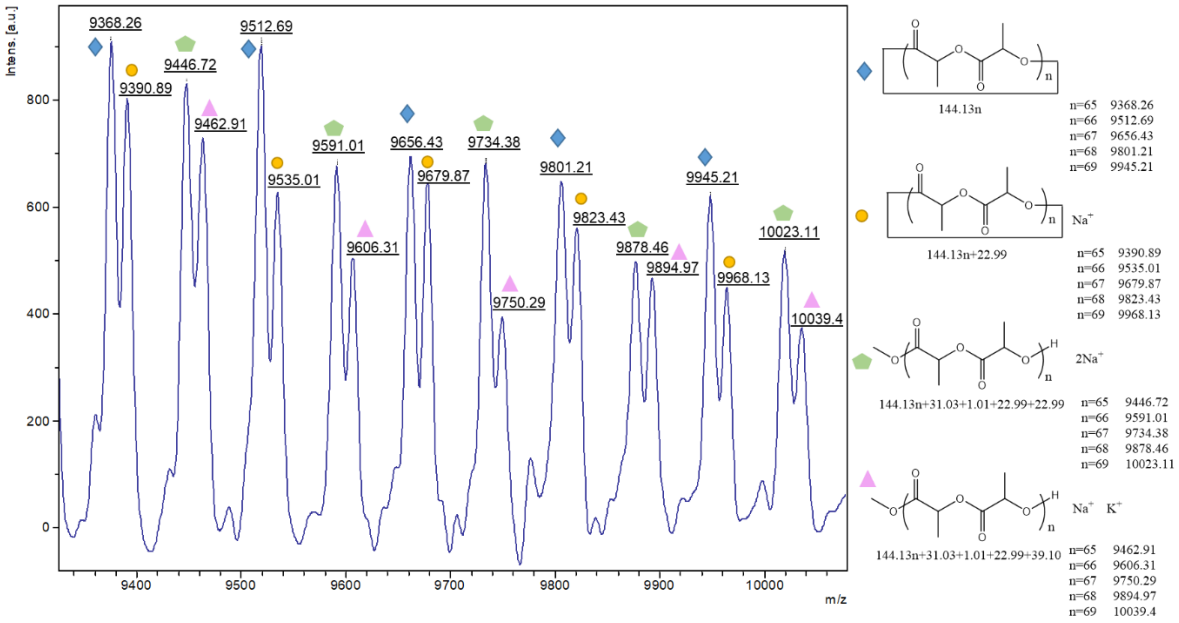

Figure S32. MALDI-TOF spectrum of PLA using **1** (Table 3, entry 1).

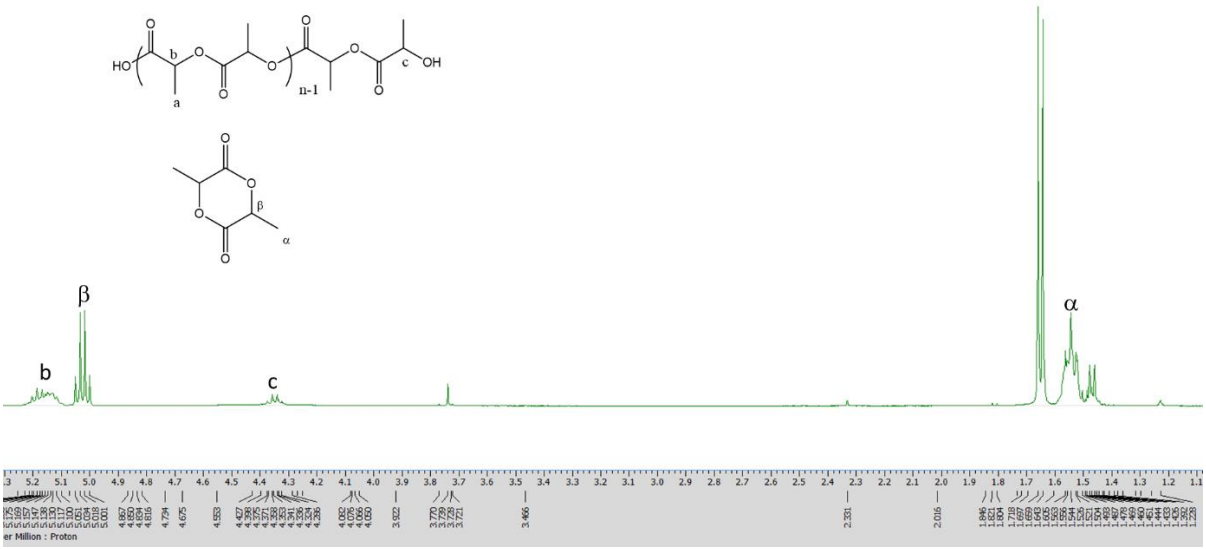

Figure S33. ^{1}H NMR (400 MHz, $CDCl_3$) spectrum of PLA using **2** (Table 3, entry 2).

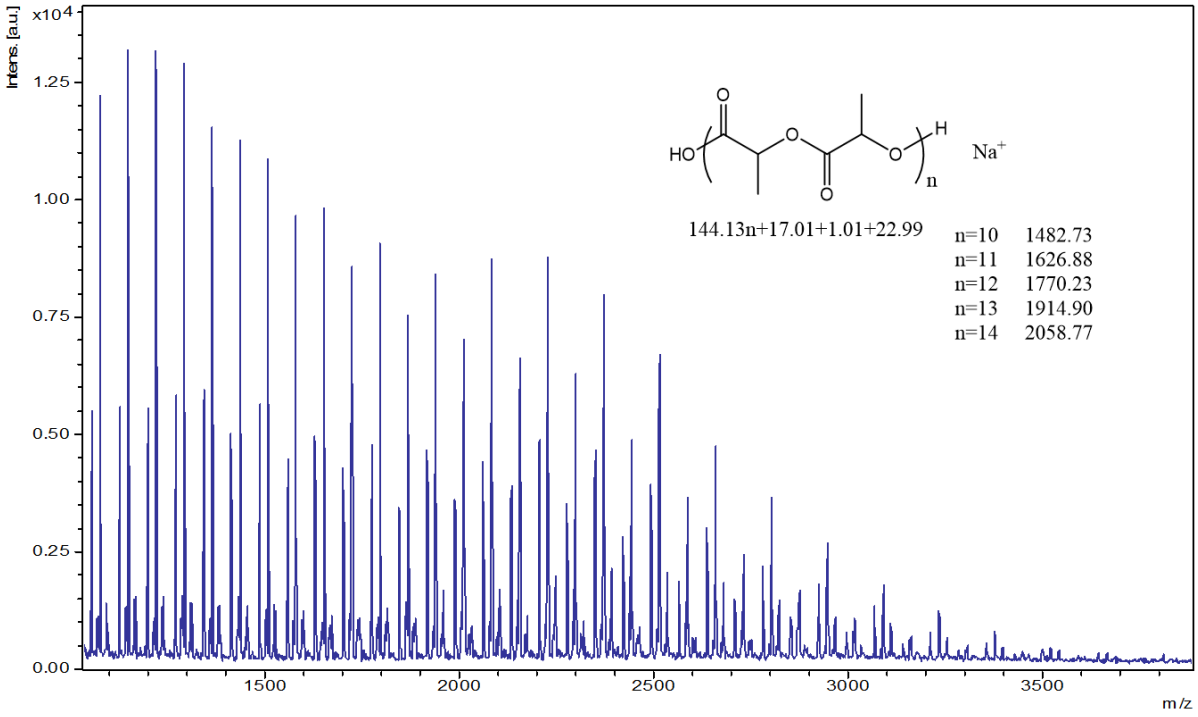

Figure S34. MALDI-TOF spectrum of PLA using **2** (Table 3, entry 2).

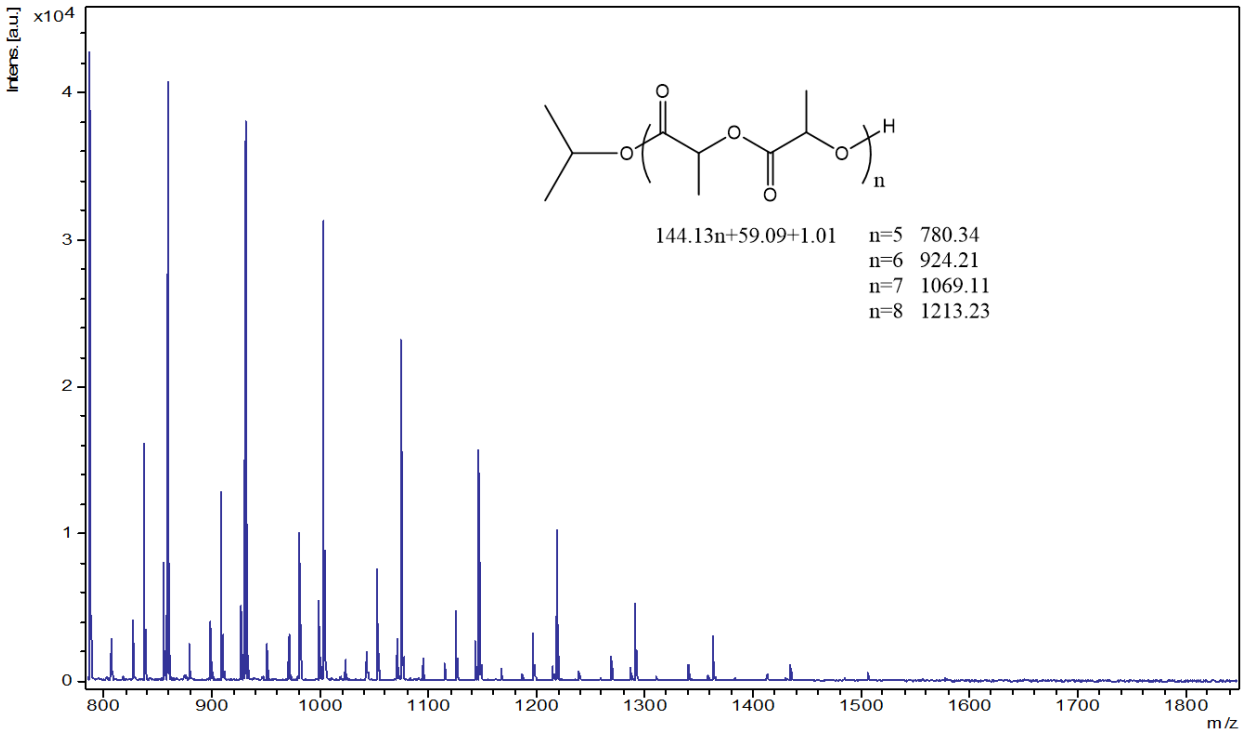

Figure S35. MALDI-TOF spectrum of PLA using **3** (Table 3, entry 3).

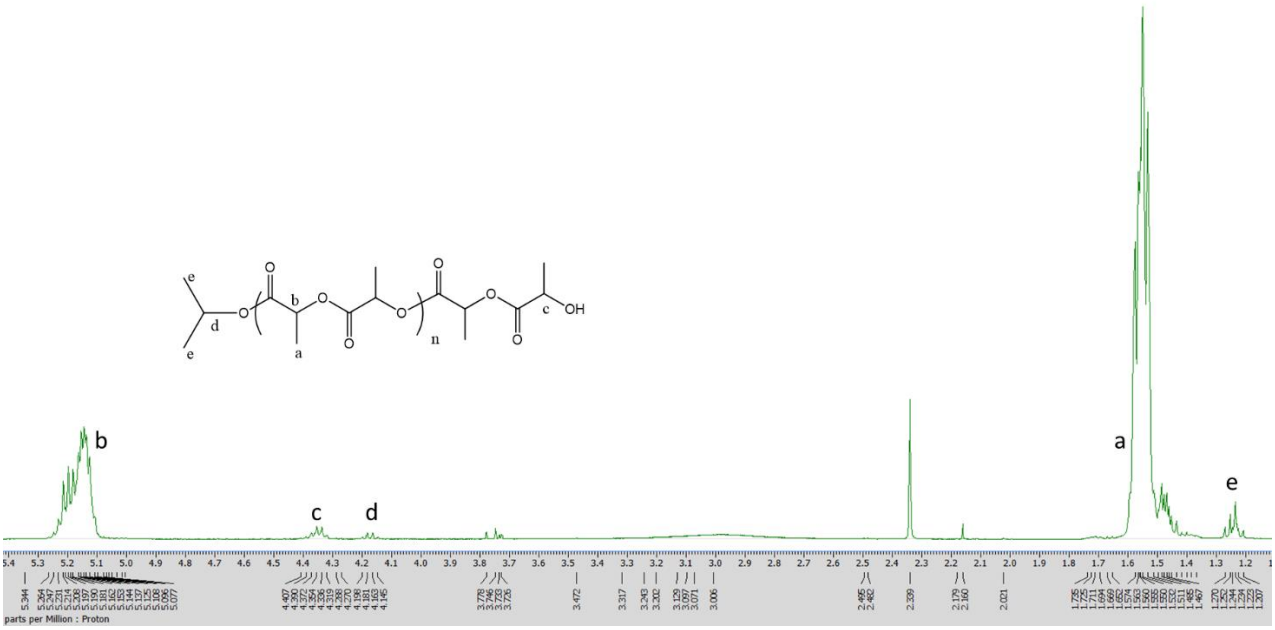

Figure S36. ^{1}H NMR (400 MHz, $CDCl_3$) spectrum of PLA using **4** (Table 3, entry 4).

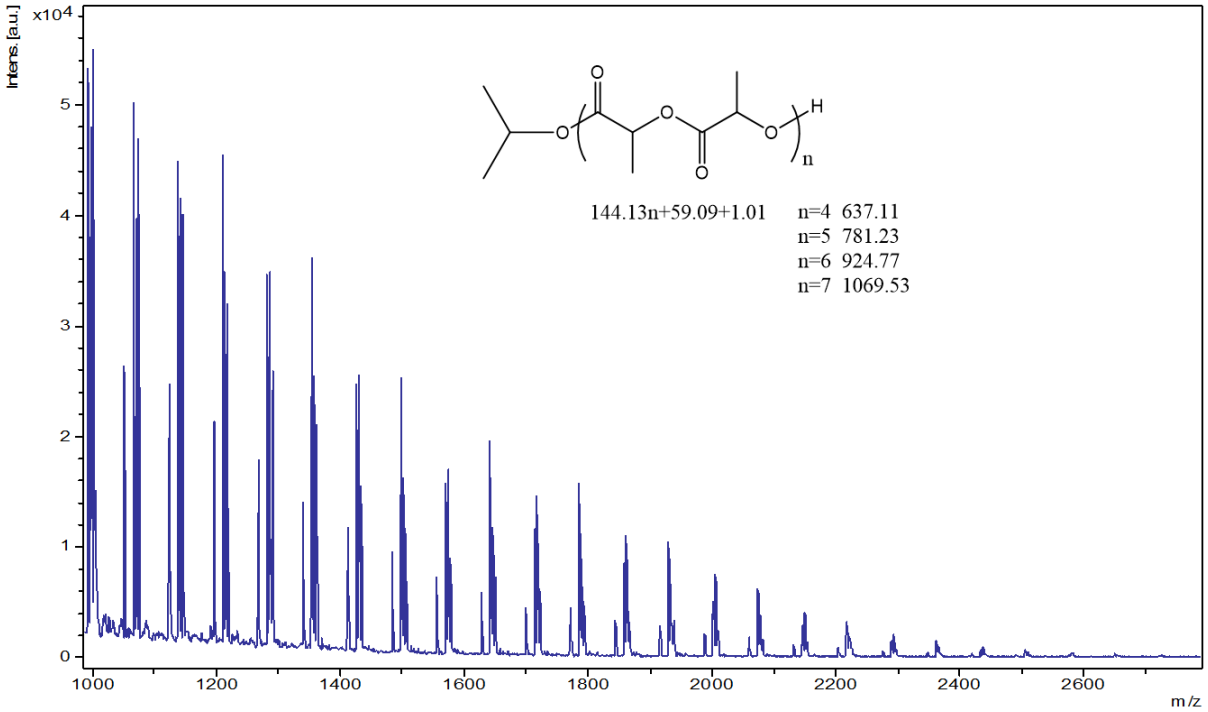

Figure S37. MALDI-TOF spectrum of PLA using **4** (Table 3, entry 4).

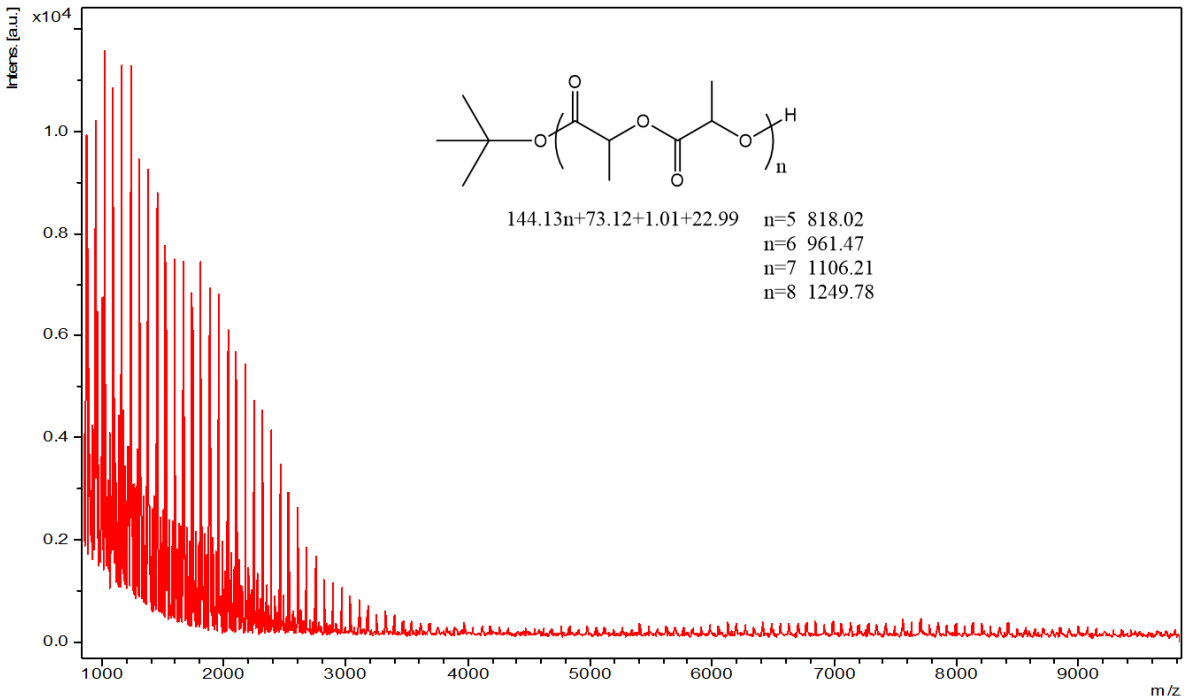

Figure S38. MALDI-TOF spectrum of PLA using **5** (Table 3, entry 5).

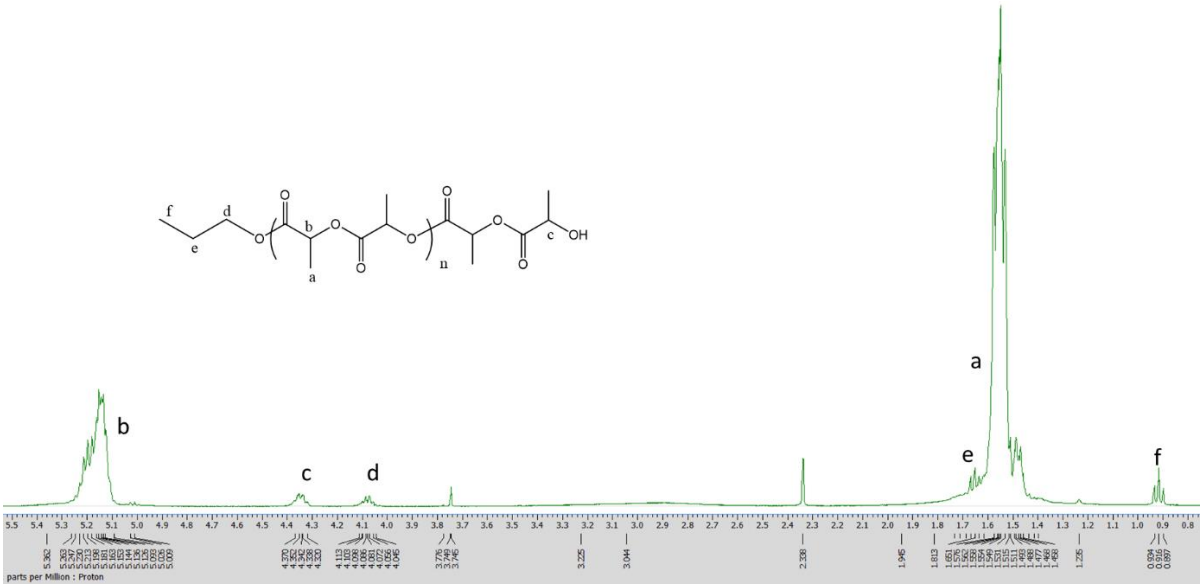

Figure S39. ^{1}H NMR (400 MHz, $CDCl_3$) spectrum of PLA using **7** (Table 3, entry 7).

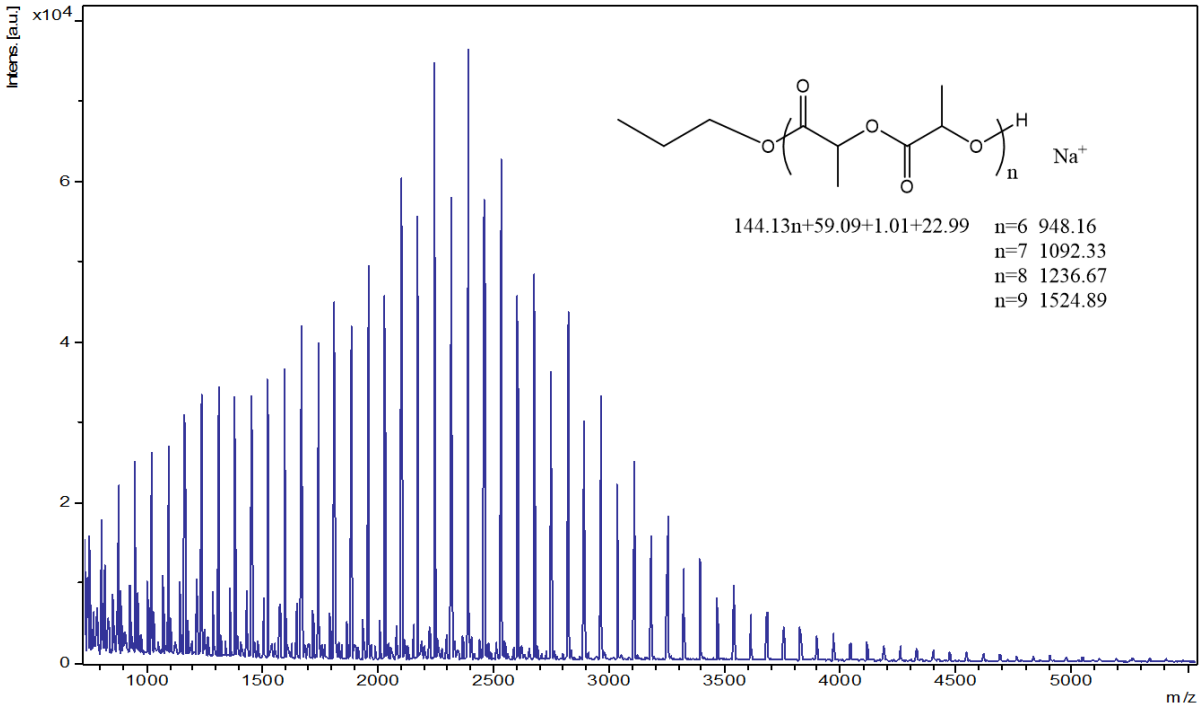

Figure S40. MALDI-TOF spectrum of PLA using **7** (Table 3, entry 7).

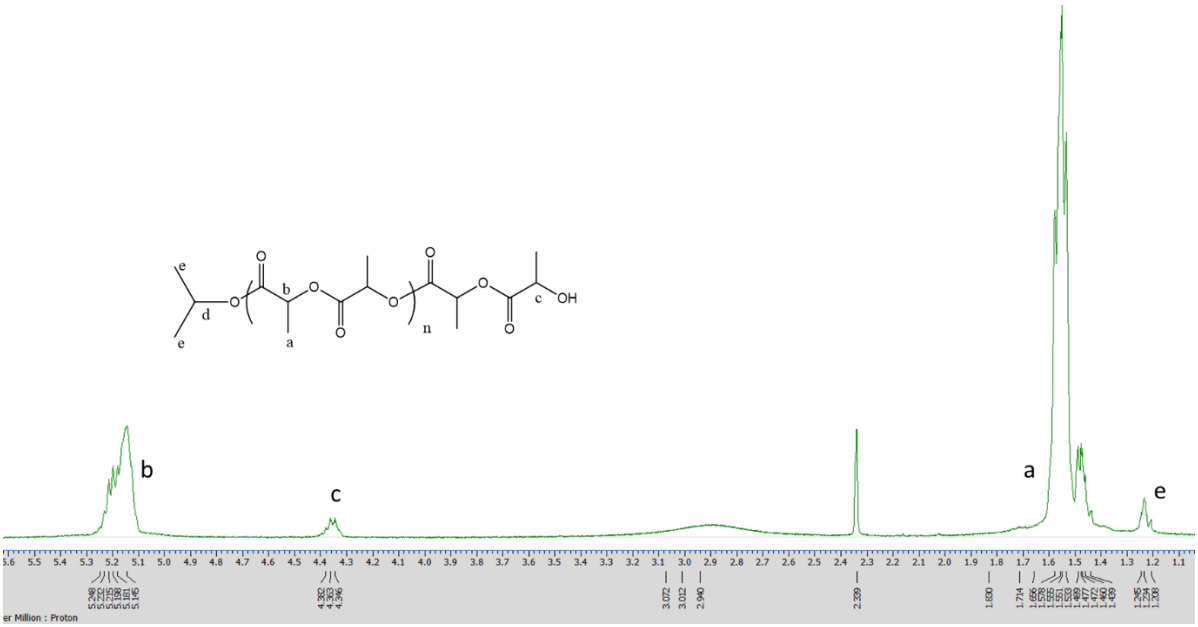

Figure S41. ^{1}H NMR (400 MHz, $CDCl_3$) spectrum of PLA using **8** (Table 3, entry 8).

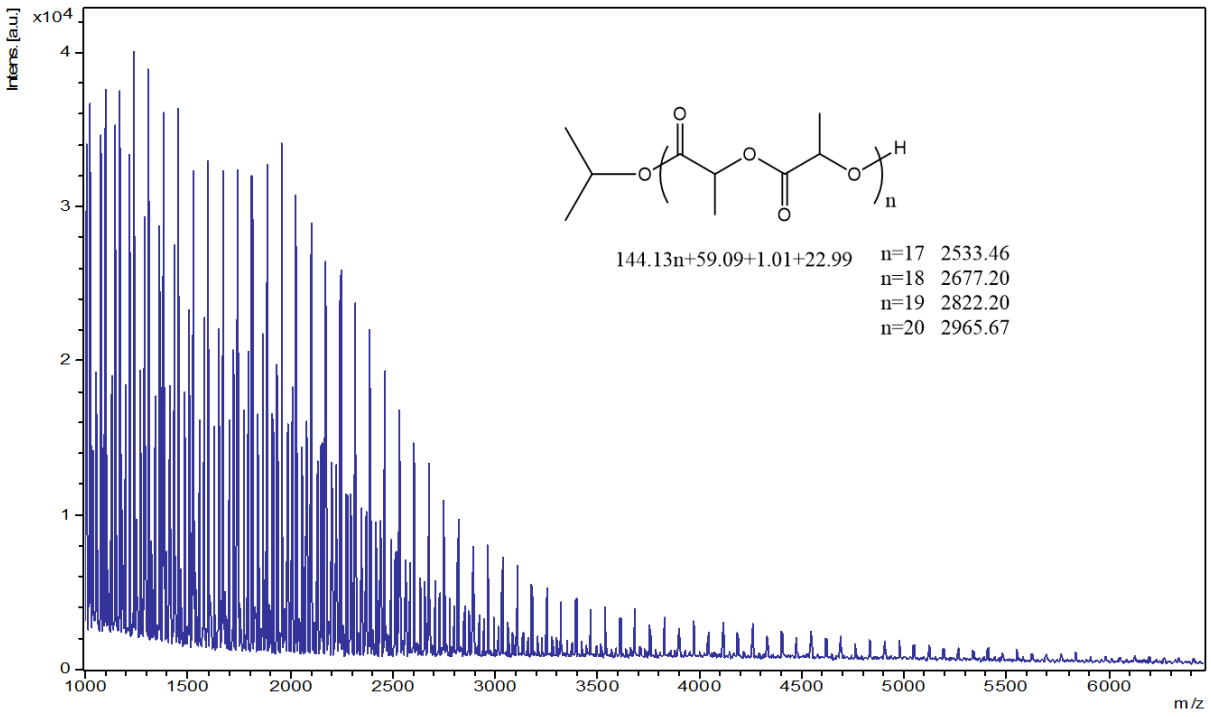

Figure S42. MALDI-TOF spectrum of PLA using **8** (Table 3, entry 8).

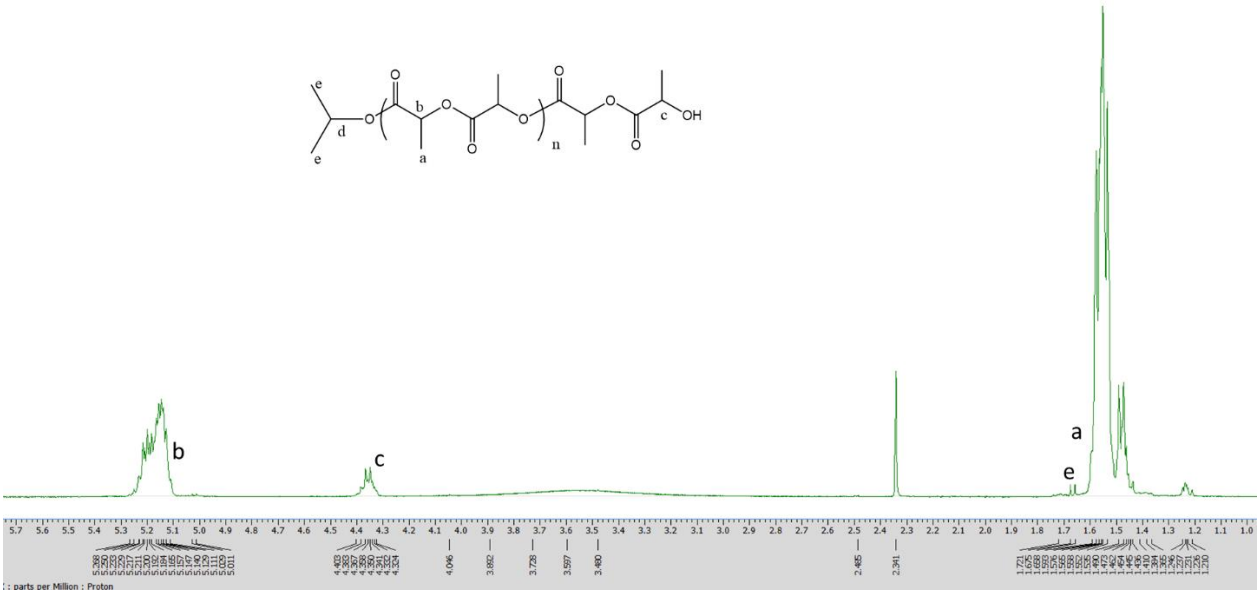

Figure S43. ^{1}H NMR (400 MHz, $CDCl_3$) spectrum of PLA using **9** (Table 3, entry 9).

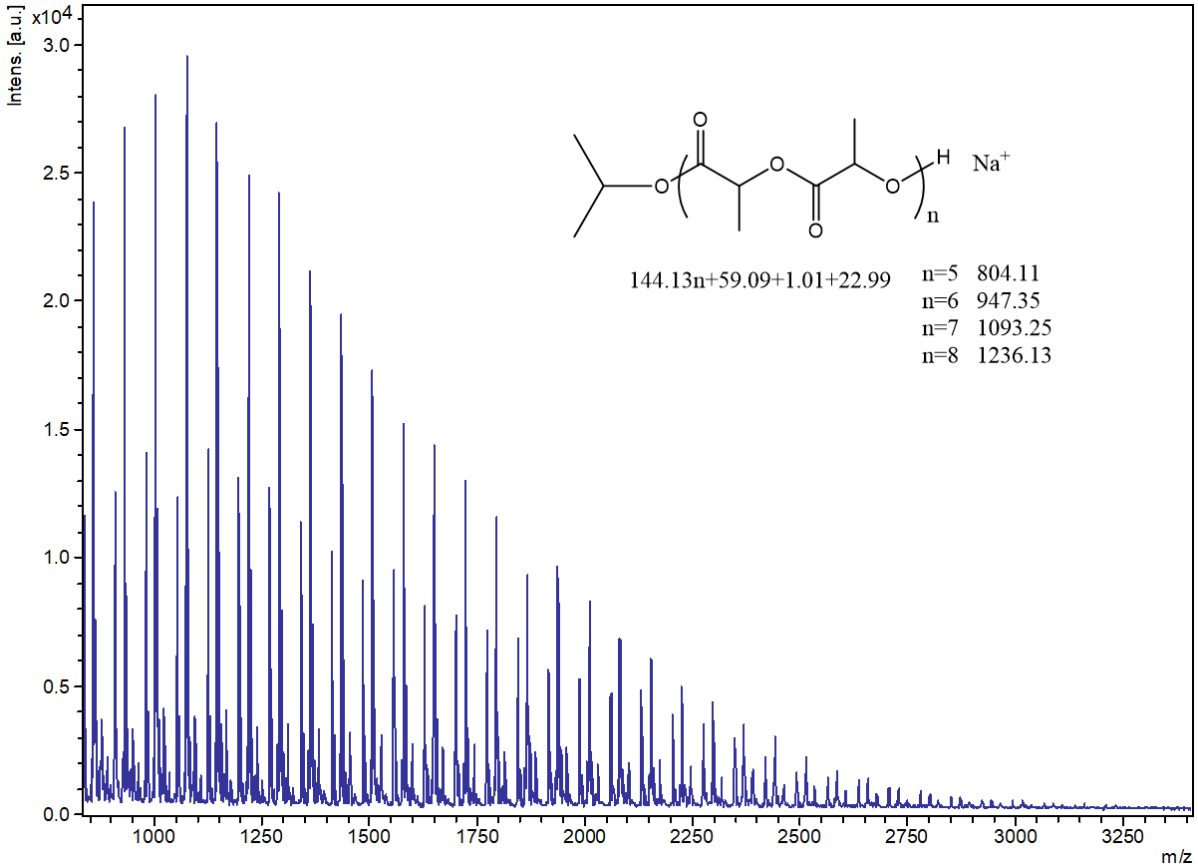

Figure S44. MALDI-TOF spectrum of PLA using **9** (Table 3, entry 9).

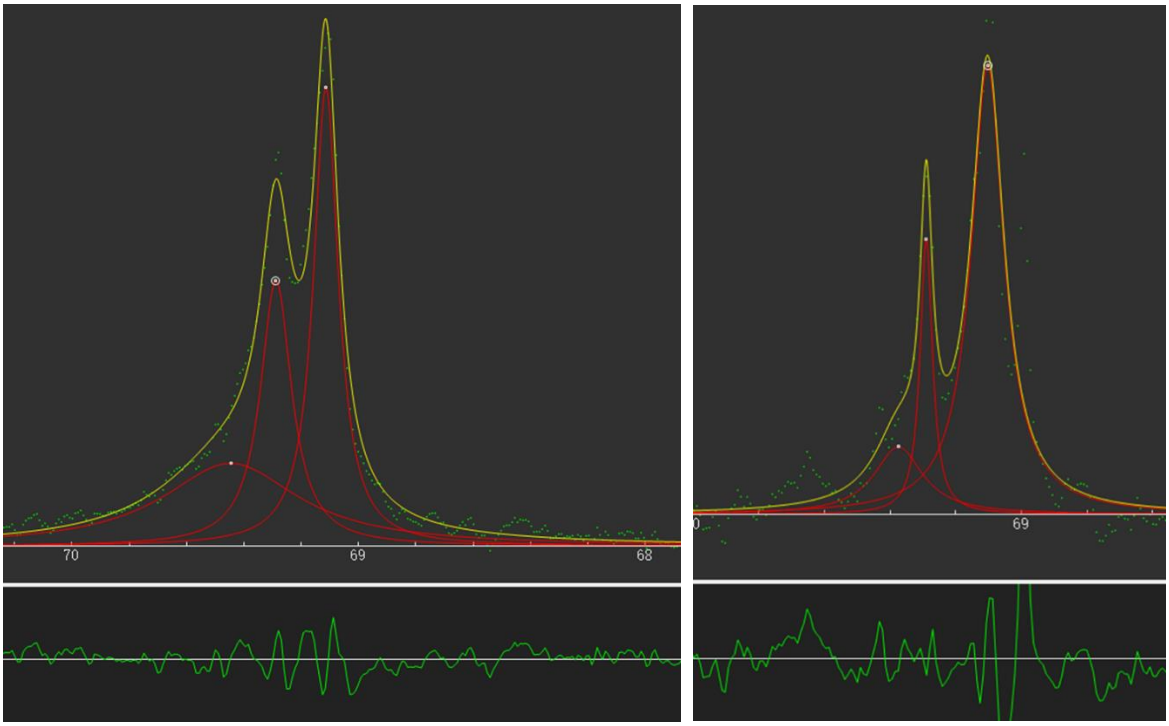

Figure S45. ^{13}C NMR spectrum of methine carbon in PLA using **1** (left) and **2** (right) (Table 3, entries 1 and 2).

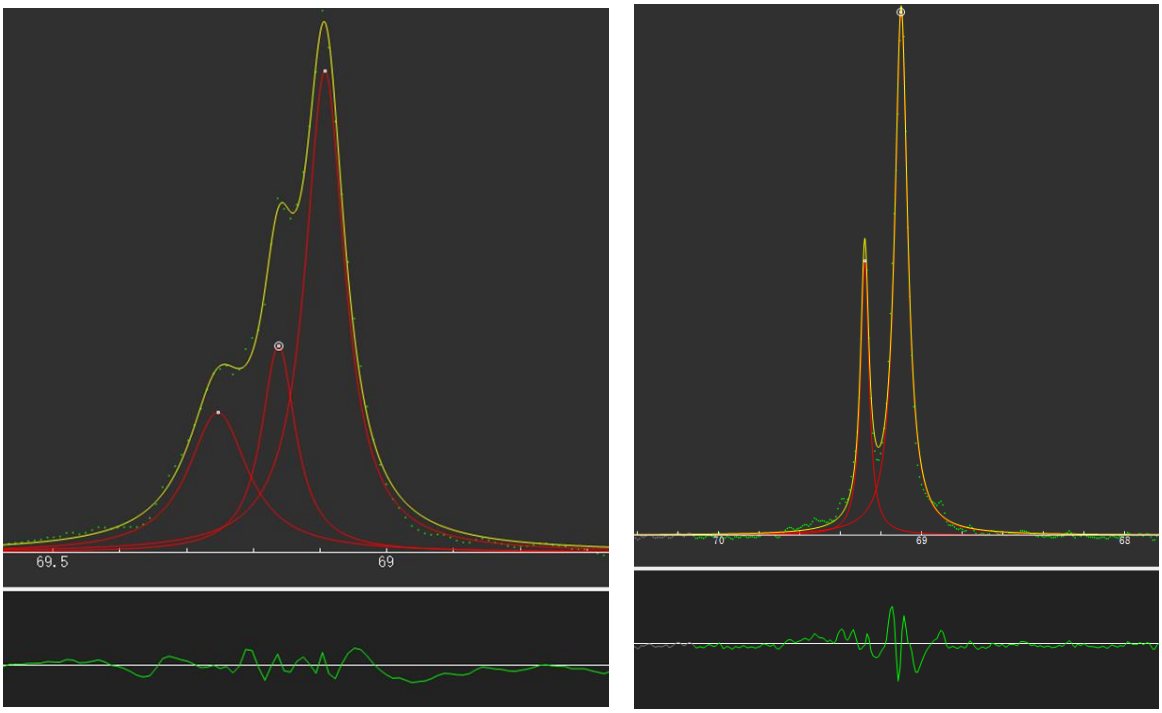

Figure S46. ^{13}C NMR spectrum of methine carbon in PLA using **3** (left) and **4** (right) (Table 3, entries 3 and 4).

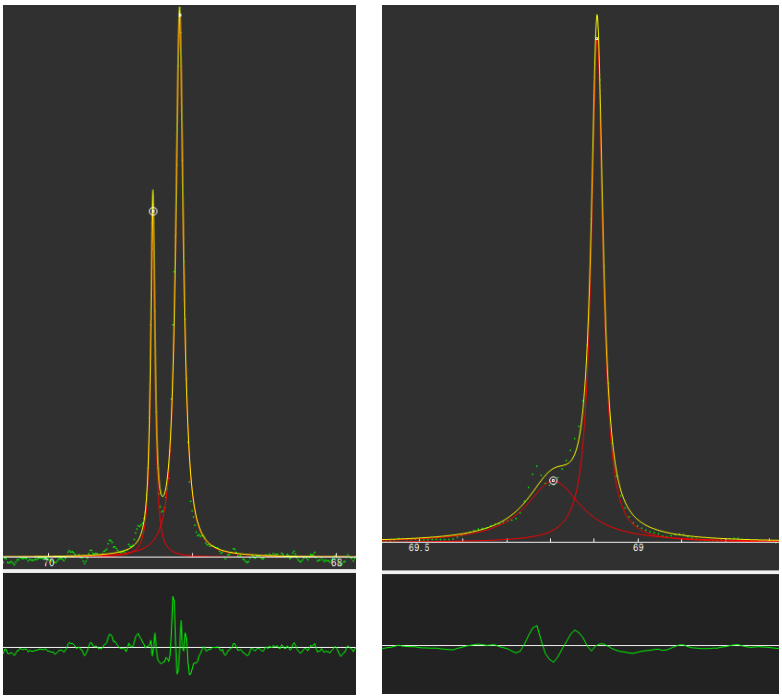

Figure S47. ^{13}C NMR spectrum of methine carbon in PLA using **5** (left) and **6** (right) (Table 3, entries 5 and 6).

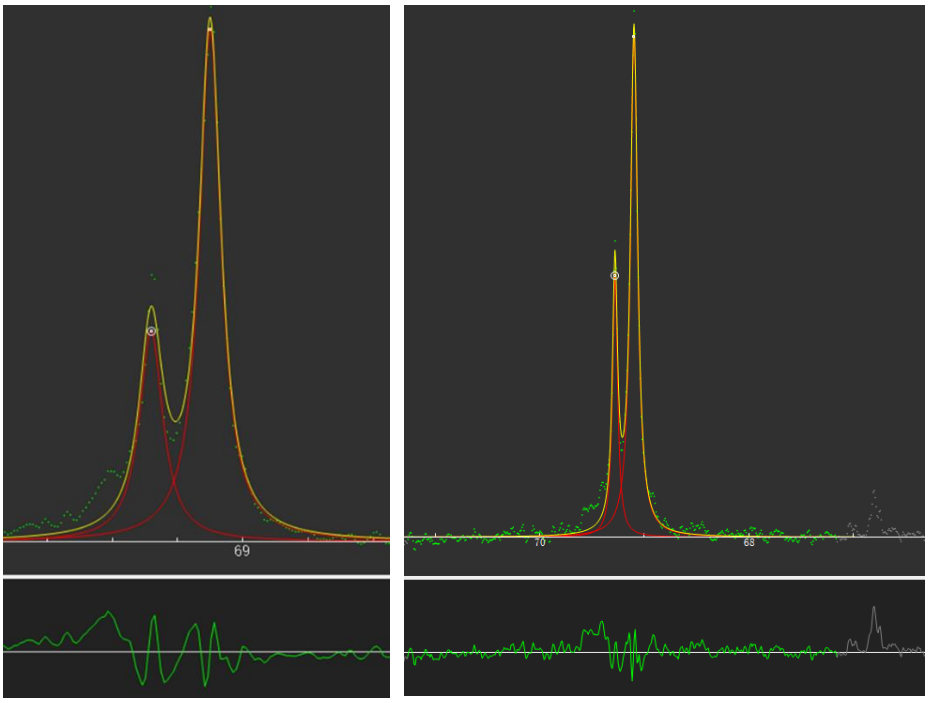

Figure S48. ^{13}C NMR spectrum of methine carbon in PLA using **7** (left) and **8** (right) (Table 3, entries 7 and 8).

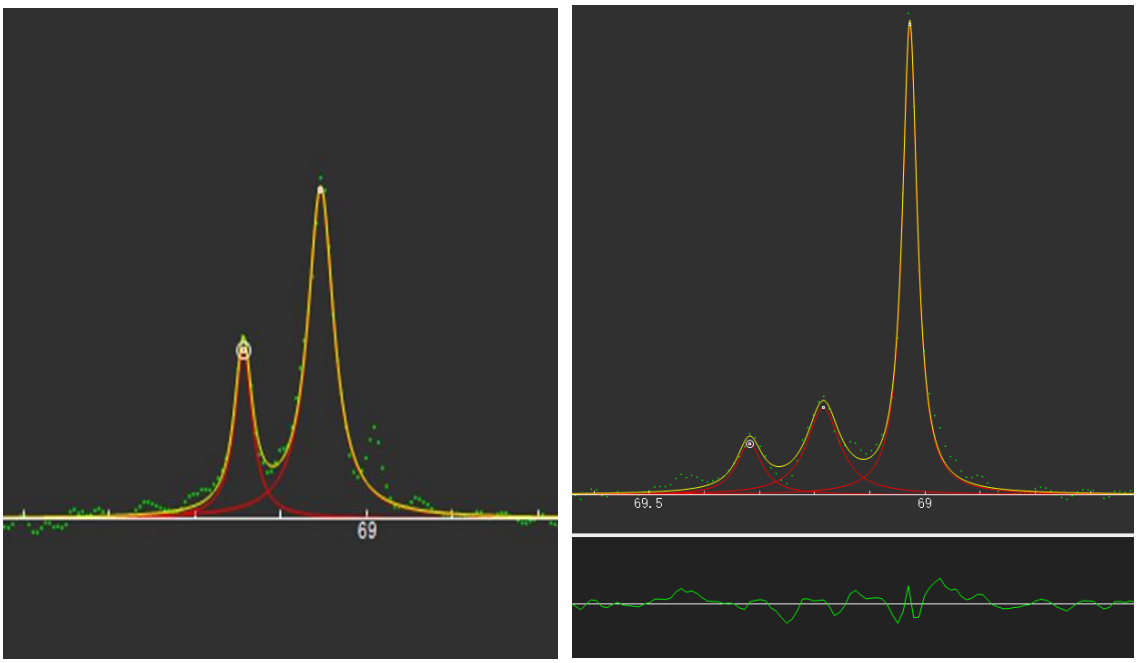

Figure S49. ^{13}C NMR spectrum of methine carbon in PLA using **9** (left) and **10** (right) (Table 3, entries 9 and 10).

References

[S1] R. A. Coxall, S. G. Harris, D. K. Henderson, S. Parsons, P. A. Tasker, R. E. P. Winpenny, *J. Chem. Soc., Dalton Trans*. 2000, 14, 2349-2356.